https://doi.org/10.5194/egusphere-2025-174
Preprint. Discussion started: 18 February 2025

Vegetation and climate changes at the Early-Late Pliocene Transition around the Mediterranean Basin: A case from the Burdur Basin in Southwestern Anatolia

Mary Robles[1], Valérie Andrieu[1], Pierre Rochette[1], Séverine Fauquette[2], Odile Peyron[2], François Demory[1], Oktay Parlak[3], Eliane Charrat[4], Belinda Gambin[5], Mehmet Cihat Alçiçek[6]

[1] Aix-Marseille Univ., CNRS, IRD, INRAE, UM 34 CEREGE, Aix-en-Provence, France
[2] Univ. Montpellier, CNRS, IRD, EPHE, UMR 5554 ISEM, Montpellier, France
[3] Mineral Research and Exploration General Directorate, Ankara, Türkiye
[4] Aix-Marseille Univ., CNRS, IRD, INRAE, IMBE, Aix-en-Provence, France
[5] University of Malta, Institute of Earth Systems, Msida, Malta
[6] Pamukkale University, Department of Geology, Denizli, Türkiye

Correspondence to: Mary Robles (mary.robles@umontpellier.fr)

Abstract

The Pliocene (5.33-2.58 Ma), particularly the Early-Late Pliocene transition (~3.6 Ma), is a key period for understanding future climate change linked to increases in greenhouse gases. Around the Western Mediterranean Basin, the Early-Late Pliocene transition was marked by the establishment of a Mediterranean climate with summer droughts, cool/wet winters and latitudinal gradients. However, environmental changes in the eastern part of the Mediterranean area during the Early-Late Pliocene transition have rarely been documented. Here, we propose to reconstruct the environmental and climate changes during the Early-Late Pliocene transition from the Lake Burdur sequence, located in Southwestern Türkiye. The aim of this study is to characterize the vegetation, lake dynamics, and water level changes based on pollen and Non-Pollen Palynomorph (NPP) proxies, to quantitatively reconstruct climate changes using a multimethod approach (Modern Analogue Technique, Weighted Averaging Partial Least Squares regression, Random Forest, and Boosted Regression Trees and Climatic Amplitude Method) and morphologically characterize the large pollen grains of Poaceae (*Cerealia*-type).

The results indicate that, during the Early-Late Pliocene transition at Burdur, the vegetation was dominated by steppes with Poaceae, *Artemisia*, and Amaranthaceae. Subsequently, arboreal taxa decreased and a alternation between steppe grasslands with deciduous *Quercus* and steppes dominated by Amaranthaceae became evident. Large Poaceae pollen grains (*Cerealia*-type) are recorded in the Burdur sequence, but their percentages are lower than those at Acıgöl, a nearby record dated to the Pleistocene. The morphological characteristics of these large Poaceae pollen grains from Burdur are similar to those of domesticated cereals from recent periods, preventing a clear distinction between wild and domesticated Poaceae pollen. The lacustrine ecosystem was characterized by semi-aquatic vegetation and freshwater algae, exhibiting alternating oligotrophic and eutrophic conditions. Climate reconstructions of Burdur show similar trends across different methods, with reconstructed values during the Early-Late transition being close to present-day values. Following a climatic optimum in precipitation and temperature, climate reconstructions indicate an alternation between cool, wet conditions and warmer, drier conditions during the Late Pliocene in Southwestern Anatolia. Around the Mediterranean Basin, climate reconstructions during the Early Pliocene show warmer conditions compared to modern values and a north-south gradient in terms of precipitation, with wetter conditions in the north in comparison to the south. The Late

https://doi.org/10.5194/egusphere-2025-174
Preprint. Discussion started: 18 February 2025

Pliocene is characterized by colder conditions, and more humid conditions in the Western Mediterranean, while Türkyie and Central Asia experienced more arid conditions.

Keywords

Mediterranean region; Pliocene; Palynology; Paleoclimate; Transfer functions; Poaceae

1. Introduction

The Pliocene Epoch (5.33-2.58 Ma), considered a warmer period compared to the pre-industrial era, is particularly important for understanding future climate change due to the many similarities it shares with the Earth's present-day physical characteristics (Haywood et al., 2016). During warm periods of the Pliocene, atmospheric CO_2 concentration are estimated to have reached 350-450 p.p.m.v. (Raymo et al., 1996; Pagani et al., 2010), the Northern and West Antarctic ice sheets were smaller (Brierley et al., 2009; Fedorov et al., 2013), and sea levels were significantly higher than today (Dowsett and Cronin, 1990; Miller et al., 2012). General Circulation Model (GCM) simulations suggest that the average temperature during the Late Pliocene (3.2-3 Ma) was approximately 3°C higher than in the pre-industrial era. This temperature increase was particularly pronounced in the Northern Hemisphere high latitudes, where mean annual temperatures reached as high as 18°C (Haywood et al., 2013, 2020; Salzmann et al., 2013; Panitz et al., 2016). The Pliocene is divided into two periods (Haywood et al., 2016): (1) the Early Pliocene (Zanclean Age; 5.3-3.6 Ma), a warm period primarily characterized by 19-23 ka oscillations linked to precession orbital cycles, and (2) the Late Pliocene (Piacenzian Stage; 3.6-2.58 Ma) a generally colder period dominated by 19-23 ka and 41 ka oscillations linked to precession and obliquity orbital cycles (Haywood et al., 2009). The decrease in temperatures led to the initiation of the Northern Hemisphere glaciation from 3.6 to 2.4 Ma (Mudelsee and Raymo, 2005). Moreover, two major cooling events are evidenced at the Early-Late Pliocene transition, the MIS MG12 at ~3.58 Ma and the MIS M2 at ~3.3 Ma (Lisiecki and Raymo, 2005; De Schepper et al., 2014).

The Early Pliocene was characterized by Mediterranean climate conditions (summer droughts and cool-wet winters) around the Mediterranean Basin, while Northern and Central Europe experienced more pronounced continental conditions (Suc, 1984; Suc et al., 2018). This contrasting seasonality of the Mediterranean climate became established after the MIS M2 glacial event at ~3.3 Ma (Lisiecki and Raymo, 2005; Bertini, 2010; Jiménez-Moreno et al., 2010; De Schepper et al., 2014). At that time, the temperatures are estimated to have been 3 to 6°C higher than modern values in the Western Mediterranean region (Fauquette et al., 2007). In terms of precipitation, a north-south gradient has been identified, with higher than modern precipitation levels in Northwestern Europe and values similar to modern levels in Southwestern Europe (Fauquette et al., 2007). In contrast to the western areas, the climate of the Eastern Mediterranean region remains poorly documented.

At the Early-Late Pliocene transition (~3.6 Ma), the vegetation of Western Europe, inferred from numerous pollen data (Suc et al., 1995; Fauquette et al., 2007; Jiménez-Moreno et al., 2010; Combourieu-Nebout et al., 2015; Suc et al., 2018 and references herein) was characterized by a clear latitudinal gradient. In Northwestern Europe, vegetation was dominated by taxa adapted to year-long wet climates, particularly during the Early Pliocene. However, a reduction in mega-mesothermic taxa, such as *Engelhardia* and *Taxodium*-type, is observed during the Late Pliocene. In the Northwestern Mediterranean region, mega-mesothermic taxa were still represented during the Late Pliocene, but there was a general increase, compared to the Early Pliocene, in

https://doi.org/10.5194/egusphere-2025-174
Preprint. Discussion started: 18 February 2025

deciduous mesothermic (e.g. deciduous *Quercus*) and Mediterranean sclerophyllous plants (e.g. *Quercus ilex*-type) which are better adapted to a dry season. In contrast, the Southwestern Mediterranean region's vegetation resembled that of the Early Pliocene, characterized by open, steppe-like environments and warm, dry conditions. Unlike the Western Mediterranean, data from the eastern part of the region are limited, with only two palynological records available for the Early-Late Pliocene: one from the Black Sea (DSDP site 380; Popescu et al., 2010) and the other from Ericek Southwestern Türkiye (Jiménez-Moreno et al., 2015). However, the Ericek record covers only the end of the Early Pliocene. These records indicate that, prior to the transition at 3.6-3.4 Ma, forests composed of mesothermic elements developed along the Black Sea coast (Popescu et al., 2010), while steppe vegetation dominated by *Artemisia* was prevalent on the Anatolian plateau (Jiménez-Moreno et al., 2015). After 3.4 Ma, both records document the presence of open environments (Popescu et al., 2010; Jiménez-Moreno et al., 2015).

The sediment core from Lake Burdur, located in Southwestern Türkiye (ca 30 km west of Lake Acıgöl); previously dated with paleomagnetism by Özkaptan et al. (2018), represents a key record for reconstructing vegetation and climate dynamics in the Eastern Mediterranean region during the Pliocene, as well as for exploring the early development of large pollen grains of Poaceae (proto-cereal). The Eastern Mediterranean is an interesting area to document the history of Poaceae, a key taxon in Mediterranean vegetation and in a region where the development of agricultural activities emerged from the Neolithic (Brown et al., 2009; Willcox et al., 2009). Importantly, large Poaceae pollen grains have been recorded on the Anatolian plateau (Lake Acıgöl) during the Pleistocene between 2.3 and 1 Ma, with their sizes ranging from 40 to 60 µm and their percentages representing up to 7% of the pollen signal (Andrieu-Ponel et al., 2021). For grains larger than 45-50 µm, Poaceae pollen identification keys assign these grains to domesticated cereals (Andersen, 1979; Tweddle et al., 2005; Joly et al., 2007; Muller et al., 2022). Nevertheless, large Poaceae pollen grains dated to the Pleistocene and exceeding 45–50 µm in size, are found well before the emergence of agricultural activities (Andrieu-Ponel et al., 2021). Andrieu-Ponel et al. (2021) refer to them as proto-cereals, linking the appearance of such pollen to the pressure exerted by large herds of herbivores on steppe ecosystems around Lake Acıgöl, leading to genetic mutations in Poaceae. This question is complex, and within this context, it would be particularly valuable to investigate the presence of pollen from proto-cereals in other, older time periods such as the Early-Late Pliocene transition.

Here we propose to address this gap in the Eastern Mediterranean by documenting environmental changes during the Early-Late Pliocene transition using the Lake Burdur core. Our specific aims are to:

1) Reconstruct vegetation and lake dynamics based on pollen and Non-Pollen Palynomorphs (NPPs),
2) Quantitatively reconstruct climate changes using a multi-method approach, including the Modern Analogue Technique, Weighted Averaging Partial Least Squares regression, Random Forest, and Boosted Regression Trees and Climatic Amplitude Method,
3) Morphologically characterize large pollen grains of Poaceae (*Cerealia*-type).

2. Study site

2.1 Geographical, geological and hydrological settings

The Anatolian peninsula is defined by a high central plateau (ca. 1000–1200 m a.s.l.), surrounded by mountain ranges in the north, including the Pontic chain, and in the south by the Taurus Mountains (Kuzucuoğlu, 2019). The southwestern region of Anatolia, called the "Lake District", is characterized by nine large lakes, and

https://doi.org/10.5194/egusphere-2025-174
Preprint. Discussion started: 18 February 2025

several small lakes, most of which are tectonic in origin although some are karstic (Bering, 1971). The altitudes of these lakes are around 850-1100 m a.s.l and they are surrounded by mountains with peaks above 2500 m. The largest lakes include freshwater (Beyşehir and Eğirdir), saline (Akşehir and Burdur) and hypersaline conditions (Acıgöl and Salda), with the majority of lakes in this region considered endorheic (Kuzucuoğlu, 2019).

Southwest Anatolia (Fig. 1) is characterized by three structural units: the basement Bey Dağları autochthon and tectonically overlain Antalya and Lycian nappes collectively forming the Tauride Orogeny, which resulted from the closure of the Neotethys Ocean during the Mesozoic-Early Cenozoic (ten Veen et al., 2009). Following the culmination of the Taurides in Southwestern Anatolia, a regional crustal extension occurred from the Late Miocene onwards, resulting in a broad array of NE-trending, normal-fault bounded orogen-top basins hosting contemporaneous alluvial-fan, fluvial and lacustrine deposits (Alçiçek et al., 2019).

The Burdur Basin, hosting Lake Burdur (37°43'2.748"N, 30°9'14.792"E, 845 m a.s.l.), is one of these orogen-top basins controlled by a NE-trending master-fault and filled by Late Miocene-Early Pleistocene alluvial-fan, fluvial and lacustrine deposits (Price and Scott, 1991; Alçiçek et al., 2013; Fig. 1). The lake spans 27 km by 8 km, with an average depth of 60 to 80 m and a maximum depth of 110 m; anoxic zones are present in these deeper areas (Çolak et al., 2022). Lake Burdur is an endorheic lake characterized by alkaline conditions with high salinity and elevated ion concentration, this is because evaporation is not compensated by hydrological inputs, leading to the accumulation of salts and ions in the water (Çolak et al., 2022). The lake receives water from seasonal and perennial rivers (55%), precipitation (40%) and groundwater (5%) (Çolak et al., 2022; Dervişoğlu et al., 2022). Since 1974, dams and reservoirs have been built for domestic use and agricultural irrigation along nearly all the rivers that feed into the lake, leading to a lake volume decrease of 39% between 1975 and 2016 (Davraz et al., 2019).

https://doi.org/10.5194/egusphere-2025-174
Preprint. Discussion started: 18 February 2025

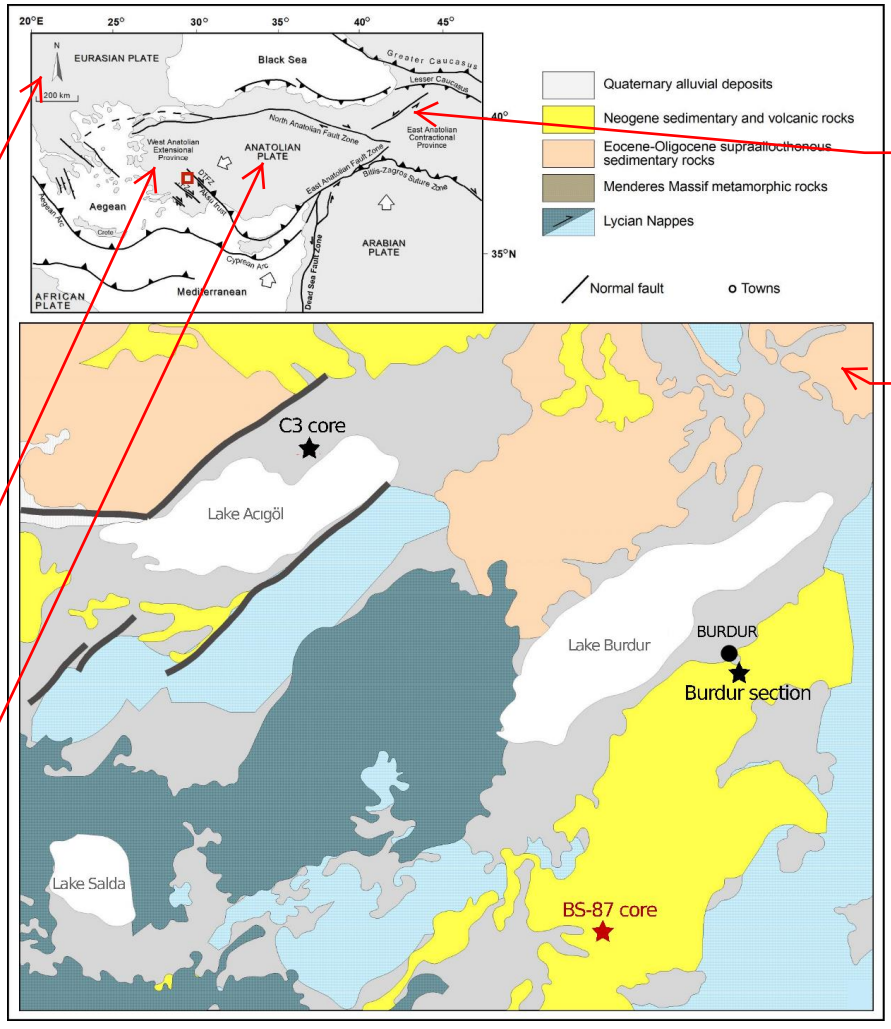

Figure 1: Geological maps of Burdur Province and locations of selected cores and sections: C3 core (Andrieu-Ponel et al., 2021), Burdur section (Özkaptan et al., 2018) and BS-87 core (this study).

2.2 Present-day climate and vegetation

The topographic barriers created by the Taurus Mountains block southerly and south-westerly airflows, leading to climate variability, distinct ecological conditions, and a high numbers of endemic species (Medail and Quézel, 1997). The Burdur province is characterized by a Mediterranean climate with hot-dry summers and cool-wet winters according to the Köppen-Geiger climate classification (Kottek et al., 2006). The meteorological station of Burdur shows an annual precipitation of 593 mm with a maximum in January (80 mm) and a minimum in July and August (9 and 8 mm, respectively) between 1991 and 2021. Mean annual temperature corresponds to 12.2°C with a minimum in January (1.3 °C) and a maximum in July and August (23.7 °C) between 1991 and 2021.

Anatolia is located at the intersection between three floristic regions: Mediterranean, Euro-Siberian and Irano-Turanian, and its vegetation is among the richest in Europe (Davis et al., 1965). This region is considered a

https://doi.org/10.5194/egusphere-2025-174
Preprint. Discussion started: 18 February 2025

biodiversity hotspot and has served as a refuge for plants that were once widespread across Europe and the Mediterranean (Biltekin et al., 2015; Medail and Quézel, 1997). Specifically, Southwest Anatolia represents the boundary between two phytogeographical regions: the Mediterranean and Irano-Turanian (Davis et al., 1965). The vegetation in Southwestern Anatolia, particularly in the 'Lake District,' has been cataloged using a flora guide (Pils, 2006). Between 800 and 1200 m a.s.l., the vegetation is dominated by evergreen shrubs such as *Quercus coccifera* and *Juniperus excelsa*. Between 1200 and 1600 m a.s.l., the vegetation consists of evergreen shrubs and conifers dominated by *Juniperus excelsa, J. oxycedrus, Pinus nigra, Cedrus libani*, and *Quercus infectoria*. Above the tree-line, at around 1600 m a.s.l., the landscape is characterized by alpine meadows, home to species such as *Astragalus sp.* and *Acantholimon sp.*

3. Material and methods

3.1 Coring and core conservation

The core BS-87 series of Lake Burdur was taken in Pliocene alluvial and fluvial deposits located to southeast of the lake (Fig. 1). Drilling operations at BS-87 were carried out at 37°30'59.735"N, 30°7'59.768"E and elevation of 1064 m a.s.l. The core is 275 m long and is stored in the warehouse area of the Mineral Research and Exploration Directorate of Türkiye (MTA) in Ankara. Core sampling was undertaken in November 2019 at the warehouse site of MTA in Ankara. One sample was taken every meter when the sediment was compacted.

3.2 Paleomagnetism and magnetic susceptibility

The time span of the Lake Burdur alluvial and fluvial sedimentary succession, spanning over Pliocene and late Miocene, is primarily based on mammal paleontological constrains (zones MN11 to 17; Alçiçek et al., 2013, 2019) as well as palaeomagnetic dating (Özkaptan et al., 2018). Palaeomagnetic analyses were conducted on the 370 m long BS-87 core. Stepwise alternating-field (AF) demagnetization up to 80 mT and thermal demagnetization up to 610°C of the Natural Remanent Magnetization (NRM) were performed on 109 and 49 cubic samples of 8 cm^3, respectively. All remanent magnetizations were measured using a superconducting rock magnetometer (SRM760R, 2G Enterprises) with an in-line AF demagnetization system, whereas thermal demagnetizations were performed in a magnetically shielded oven (TD48-SC, ASC). As the core is not oriented in declination, the proposed geomagnetic polarity sequence was determined based on the inclination of the Characteristic Remanent Magnetizations (ChRM), i.e., the stable remanent magnetizations obtained after several steps of demagnetization.

Magnetic susceptibility (MS) was measured on the same samples subjected to AF demagnetization of the NRM, which were homogeneously distributed along the 370 m long section BS-87. For MS measurements, an MFK1 Susceptibility Meter (AGICO) was used with a field of 200 A/m at a frequency of 976 Hz.

3.3 Pollen and Non-Pollen Palynomorph (NPP) analyses

A total of 53 samples from the BS-87 core of Lake Burdur were collected with an average resolution of 5 m (ranging from 1.8 m to 15.7 m) for pollen analysis between 265 m and the top of the core. For each sample, 15-20 g of sediment was processed following standard palynological procedure as described by Faegri et al. (1989), Moore et al. (1991) and Nakagawa et al. (1998). Samples were treated using hydrochloric acid (HCl 37%), sodium hydroxide (NaOH 10%), sodium hexametaphosphate ($(NaPO_3)_6$), dense liquor of sodium polytungstate (LST,

https://doi.org/10.5194/egusphere-2025-174
Preprint. Discussion started: 18 February 2025

d=2), sieving (200 µm and 10 µm), acetolysis and hydrofluoric acid (HF 70%). Preparations were mounted on glass slides with glycerol-gelatine jelly. Microscopic analysis was undertaken using an Olympus BX53-P microscope at a standard magnification of 600x. Pollen and NPP taxa were identified using photo atlases (Beug, 2004; Cugny et al., 2010; Lee et al., 2022; Reille, 1998; Van Geel, 2002). Pollen of *Pinus sylvestris* and *Pinus mediterranean*-type have been differentiated based on their size, with *Pinus sylvestris* being smaller (Reille, 1998). A minimum of 300 pollen grains of terrestrial taxa, excluding aquatic plants, mainly Cyperaceae and fern spores was counted by slide to obtain a representative assessment of pollen types (Lytle and Wahl, 2005). Measurements were performed on grass (Poaceae) pollen grains greater than 40 µm on diameters of grain (the longest axis), annulus and pores (Joly et al., 2007; Tweddle et al., 2005). Aquatic taxa, fern spores, and NPPs (algae and fungal spores) were counted alongside pollen.

The pollen diagrams were constructed with the R package *Rioja* (Juggins, 2020). Terrestrial pollen taxa are expressed in percentages of total terrestrial pollen. Hygrophilous and aquatic pollen taxa are expressed in percentages of total pollen. Fern spores, algae and fungi are expressed in percentages of total terrestrial pollen and NPPs. The pollen diagrams were zoned from a cluster analysis (CONISS; Grimm, 1987) with the R package *Rioja* (Juggins, 2020). Principal component analysis (PCA) was also performed on pollen and NPP data with the R *FactoMineR 2.4* package (Lê et al., 2008).

3.4 Pollen-inferred climate reconstructions

Traditionally, 'Coexistence Approach' methods have been preferred for periods prior to the Quaternary because these methods make it possible to quantify the climate of periods for which no pollen assemblage analogs exist in the modern pollen floras such as the Pliocene. Among these methods, the Climatic Amplitude Method (CAM, Fauquette et al., 1998a) appears the most accurate to reconstruct the climate conditions from the Neogene pollen samples (e.g. Fauquette et al., 1999, 2006; Jiménez-Moreno and Suc, 2007; Jiménez-Moreno et al., 2008). CAM has been applied to the Lake Burdur pollen assemblages together with other methods, more adapted to Quaternary time periods. Such a multi-method approach is possible because the environments in the Burdur Basin, dominated by steppe taxa, are similar to present-day Mediterranean vegetation in Eastern Mediterranean (Djamali et al., 2009; Robles et al., 2022). In this context, standard methods developed for more recent times (Holocene) can be applied for the Early-Late Pliocene transition pollen samples because in Southern Europe, as subtropical taxa disappeared, they were progressively replaced by sclerophyllous Mediterranean ecosystems (Suc, 1984; Combourieu-Nebout et al., 2015; Suc et al., 2018). A multi-method approach provides greater reliability than reconstructions based on a single climate reconstruction method (Brewer et al., 2008; Peyron et al., 2005, 2011, 2013; Salonen et al., 2019).We have selected five methods: the Climatic Amplitude Method (CAM, Fauquette et al., 1998a, b), the Modern Analog Technique (MAT; Guiot, 1990), the Weighted Averaging Partial Least Squares regression (WA-PLS; ter Braak and van Dam, 1989; ter Braak and Juggins, 1993), the Random Forest (RF; Prasad et al., 2006) and the Boosted Regression Trees (Salonen et al., 2014). RF and BRT, based on machine learning, utilizes regression trees developed with ecological data, and has been used recently to reconstruct paleoclimatic changes in Northern Europe (Salonen et al., 2019, 2024) and Mediterranean Basin (Robles et al., 2023; d'Oliveira et al., 2023).

All the methods require a calibration modern pollen dataset. For the MAT, WA-PLS, RF and BRT, we use part of the Eurasian/Mediterranean pollen dataset (n = 3373 sites) compiled by Peyron et al. (2013, 2017) and completed by Dugerdil et al. (2021a) and Robles et al. (2022, 2023). A geographical constraint has been applied

https://doi.org/10.5194/egusphere-2025-174
Preprint. Discussion started: 18 February 2025

to select modern samples from Western Europe (11°W) to Turkmenistan (58°E) and from Central Europe (51°N) to North Africa (29°N). The modern pollen dataset finally selected for the calibration of these methods contains 1776 samples. These samples have been taken in six different biomes including "Cool mixed forest" (COMX), "Cool steppe" (COST), "Temperate deciduous" (TEDE), "Warm mixed forest" (WAMX), "Warm steppe" (WAST), and "Xerophytic wood/shrub" (XERO). Performance of each method and calibration training was statistically tested (Dugerdil et al., 2021) to determine how modern samples are suitable for quantitative climate reconstructions (Root Mean Square Error or RMSE and the R^2 are presented in the Supplementary Table S1). For the CAM, the dataset includes more than 8000 pollen records located in the Northern Hemisphere. The climatic estimate is obtained as a climatic range and a "most likely value", which corresponds to a weighted mean, a statistical calculation tested on modern pollen data whose R^2 and RMSE values are given in Supplementary Table S1.

Five climate parameters were reconstructed: mean annual air temperature (MAAT), mean temperature of the warmest month (MTWA), mean temperature of the coldest month (MTCO), mean annual precipitation (PANN), mean winter precipitation (Pwinter = December, January, and February) and mean summer precipitation (Psummer = June, July, August). The precipitation seasonality is not reconstructed with the Climatic Amplitude Method. For each climate parameter, the methods fitting with the higher R^2 and the lower RMSE were selected. Cyperaceae and ferns in the Burdur record have been excluded because they are associated with local dynamics. In the CAM, *Pinus* and non-identified Pinaceae (due to poor preservation of the bisaccate pollen grains) have been excluded from the pollen sum of the fossil pollen spectra (Fauquette et al., 1998b, 1999).

WA-PLS and MAT methods are applied with the R package *Rioja* (Juggins, 2020), RF is applied with the R package *randomForest* (Liaw and Wiener, 2002) and BRT with the R package *dismo* (Hijmans et al., 2021).

https://doi.org/10.5194/egusphere-2025-174
Preprint. Discussion started: 18 February 2025

In this section, a photograph and/or digital drawing of the drilling log you sampled, sample locations and sedimentological and lithological characteristics should be added. under the 4.1 or 4.2 title.

4. Results

4.1 Age-depth model

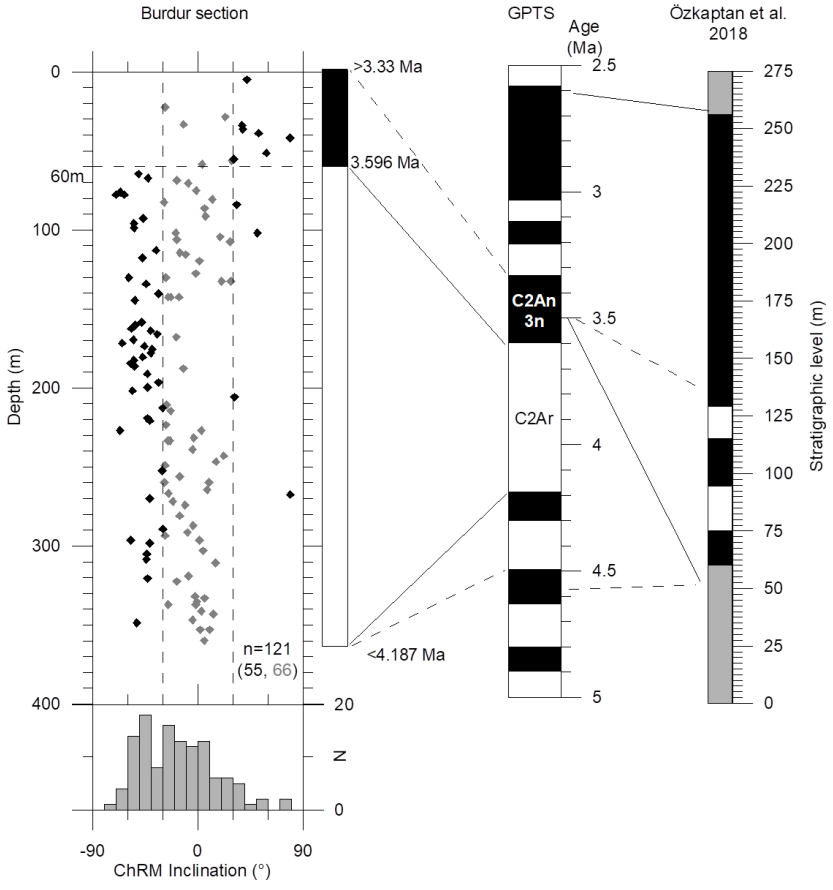

Figure 2: Magnetostratigraphic correlations of the Lake Burdur Pliocene lacustrine sediment in BS-87 core (this study; left) compared to the previously published surface section of Burdur (Özkaptan et al. 2018) with the GPTS (Hilgen et al., 2012).

Normal and reverse polarities were determined from inclination of the ChRM directions (Fig. 2). Due to different remaining overprints, the grey diamonds, showing intermediate inclinations, were only considered to support the black diamonds considered as reliable inclinations. The whole core below 60 meters depth is essentially reverse. We refrain from looking for short normal chrons, as suggested by the few normal samples in this extended reverse period, since sporadic orientation errors (e.g. upside down readings) or demagnetization issues cannot be ruled out. Above 60 meters, a clear normal chron can once again be identified.

Compared to the predominantly normal magnetostratigraphy observed 20 km to the north of our studied core (Özkaptan et al., 2018; Fig.1), the most likely identification for our long reverse chron is C2Ar. This suggests that our section lies below the northern section, with a minor overlap in C2An3n normal chron. This will be expanded on in the discussion.

https://doi.org/10.5194/egusphere-2025-174
Preprint. Discussion started: 18 February 2025

Poaceae is not steppic. Please move it in other herb.

How did you distinguish between Amaranthaceae and Chenopodiaceae? Should they be written together?

please added NAP

The values you interpret in the figure are not understood. It would be good to give counts as supplemantt ery data.

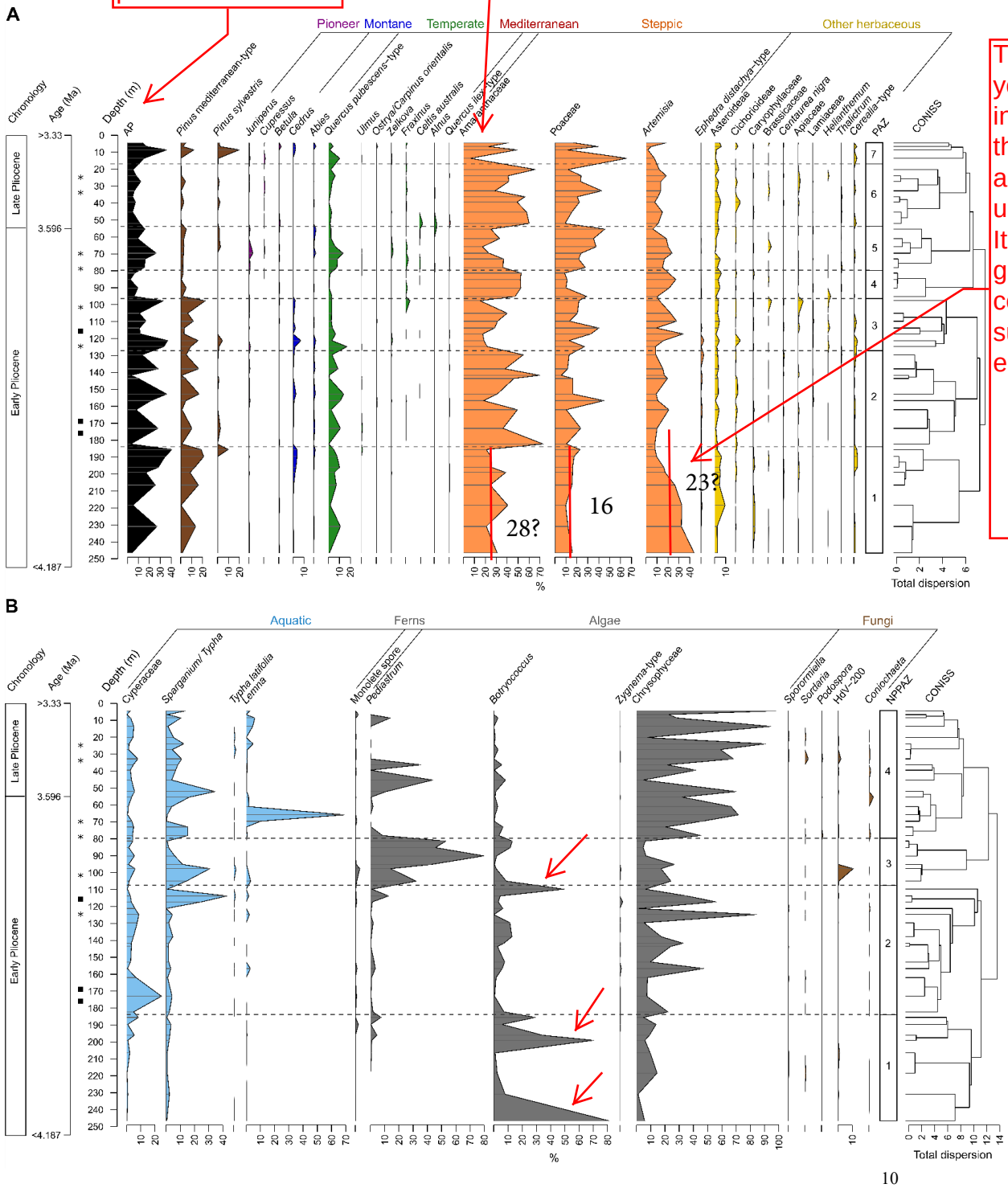

https://doi.org/10.5194/egusphere-2025-174
Preprint. Discussion started: 18 February 2025

Figure 3: Synthetic pollen diagrams from Burdur Basin (Türkiye) against core depth. A) Selected terrestrial pollen taxa, expressed as percentages of total terrestrial pollen. AP: Arboreal Pollen. PAZ: Pollen Assemblage Zones. B) Selected hygrophilous and aquatic pollen taxa and NPPs. Aquatic pollen taxa are expressed in percentages of total pollen. Fern spores, algae and fungi are expressed in percentages of total terrestrial pollen and NPPs. NPPAZ: Non-Pollen Palynomorph Assemblage Zones. Black rectangles indicate levels with macroscopic charcoal or wood. Black stars indicate very organic levels with shells.

Table 1: Description of arboreal, herbaceous, hygrophilous pollen and Non-Pollen Palynomorphs (NPPs) of Burdur core (Türkiye) against depth and age. PAZ: Pollen Assemblage Zones. NPPAZ: Non-Pollen Palynomorph Assemblage Zones. AP: Arboreal Pollen.

	Age (Ma)	Depth (m)	PAZ	Total of AP %	Herbaceous pollen types (HPT) Arboreal pollen types (APT)	NPPAZ	Hygrophilous pollen NPPs
Late Pliocene	<4.187	17-4	7	21	HPT: Poaceae (33%), Amaranthaceae (21%), *Artemisia* (8%) APT: *Pinus mediterranean*-type, *P. sylvestris*, *Quercus pubescens*-type, *Cedrus*	4	Semi-aquatic: Chrysophyceae (well-developed vegetation) Green algae: *Pediastrum* (~45 m and ~10 m), *Lemna* (~65 m), low *Botryococcus* Fungal spores: *Sordaria*, *Podospora*, Coniochaeta
		54-17	6	6	HPT: Amaranthaceae (50%), Poaceae (21%), *Artemisia* (13%)		
Early Pliocene	3.596	80-54	5	17	HPT: Poaceae (32%), Amaranthaceae (29%), Artemisia (17%) APT: *Quercus pubescens*-type, *Pinus* mediterranean-type, *P. sylvestris*, *Juniperus*, *Abies*, *Zelkova*, *Fraxinus*		
		96-89	4	6	HPT: Amaranthaceae (51%), *Artemisia* (19%), Poaceae (15%)	3	Green algae: *Pediastrum*, *Botryococcus* Semi-aquatic: *Sparganium/Typha*, Chrysophyceae Fungal peak: type HdV-200 at 100 m
		127-96	3	22	HPT: Amaranthaceae (25%), Poaceae (24%), *Artemisia* (13%) APT: *Pinus* mediterranean-type, *Quercus pubescens*-type, *Cedrus*		
		182-127	2	17	HPT: Amaranthaceae (46%), Poaceae (17%), *Artemisia* (13%) APT: Decline of *Pinus* mediterranean-type	2	Golden algae: Chrysophyceae Semi-aquatic: Cyperaceae at start, *Sparganium/Typha* at end Green algae: *Botryococcus* decreases then increases Macroscopic charcoal or wood present
	>3.33	247-184	1	23	HPT: Amaranthaceae (28%), *Artemisia* (23%), Poaceae (16%) APT: Maximum arboreal taxa (*Pinus* mediterranean-type, *Quercus pubescens*-type)	1	Green algae: *Botryococcus* Golden algae: Chrysophyceae Semi-aquatic: Cyperaceae, *Sparganium/Typha*

https://doi.org/10.5194/egusphere-2025-174
Preprint. Discussion started: 18 February 2025

Terrestrial vegetation

A total of 53 samples were analyzed from the sequence of the lacustrine succession of the Burdur Basin-fill, among which seven samples were sterile; a total of 69 terrestrial pollen types were identified. Along the sequence, terrestrial pollen indicates an open ground vegetation dominated by steppic taxa, including Amaranthaceae (ca. 37%), Poaceae (ca. 22%), and *Artemisia* (ca. 16%). The pollen diagram (Fig. 3A) is divided into seven pollen assemblage zones (PAZ) according to the CONISS method (Table 1; Grimm, 1987). This method shows a major division in the pollen diagram at 100 cm, separating PAZ 1 to 3, which contain more arboreal pollen (ca. 20%), from PAZ 4 to 7, where the percentage of arboreal pollen is lower (ca. 13%) and can be explained by a significant decrease in *Pinus* and *Quercus*. The composition of steppic taxa varies over time, alternating between high percentages of Amaranthaceae (PAZ 1, 2, 4, 6) or Poaceae (PAZ 3, 5, 7). Dominance of Poaceae is accompanied by a rise in arboreal pollen taxa, particularly due to the increase in *Quercus pubescens*-type.

PAZ 1 (247-184 m) records an open steppic vegetation dominated by Amaranthaceae (ca. 28%), *Artemisia* (ca. 23%), and Poaceae (ca. 16%), with a relatively low percentage of trees (ca. 23%), including *Pinus* mediterranean-type and *Quercus pubescens*-type. Rare pollen types (< 5%) include: Asteroideae, Caryophyllaceae, *Cedrus*, and *Pinus sylvestris.*

PAZ 2 (184-127 m) shows a dominance of Amaranthaceae (ca. 46%), a decrease of *Artemisia* (ca. 13%), whereas Poaceae remain constant (ca. 17%). Arboreal pollen taxa also decrease slightly (17%), notably due to the decline of *Pinus* mediterranean-type. Rare pollen types include: Asteroideae, Cichorioideae, *Cerealia*-type, *Pinus sylvestris, Ephedra distachya*-type, *Cedrus,* and *Abies*.

PAZ 3 (127-96 m) is marked by an increase of Poaceae (ca. 24%) and *Artemisia* (ca. 13%) and a decrease of Amaranthaceae (ca. 25%). Arboreal pollen taxa increase slightly again (ca. 22%) due to the rise of *Pinus* mediterranean-type and *Cedrus*. Rare pollen types include: Asteroideae, *Cerealia*-type, Apiaceae, Cichorioideae, *Helianthemum*, *Pinus sylvestris*, and *Cedrus*.

PAZ 4 (96-80 m) is characterized by the net increase of Amaranthaceae (ca. 51%) and *Artemisia* (19%), while Poaceae (15%) and arboreal pollen (ca. 6%) decrease drastically. Rare pollen types include: Asteroideae, *Pinus* mediterranean-type*, Quercus pubescens*-type, and *Helianthemum*.

PAZ 5 (80-54 m) is defined by an increase of Poaceae (ca. 32%) and arboreal pollen taxa (ca. 17%), the decrease of Amaranthaceae (ca. 29%), while *Artemisia* remains constant (ca. 17%). The arboreal pollen taxa diversify with the presence of *Quercus pubescens*-type, *Pinus* mediterranean-type*, P. sylvestris*, *Juniperus, Abies, Zelkova*, and *Fraxinus*. Rare herbaceous pollen types include Asteroideae and Brassicaceae.

PAZ 6 (54-17 m) is marked, as with PAZ 4, by an increase of Amaranthaceae (ca. 50%) while Poaceae (ca. 21%), *Artemisia* (13%), and arboreal pollen (ca. 6%) decrease. Rare pollen types include: Asteroideae, *Quercus pubescens*-type, *Pinus* mediterranean-type, Cichorioideae, and Apiaceae.

PAZ 7 (17-4 m) is characterized by an increase of Poaceae (ca. 33%) and arboreal pollen taxa (ca. 21%), whereas Amaranthaceae (ca. 21%) and *Artemisia* (ca. 8%) decrease. Arboreal pollen taxa include *Pinus* mediterranean-type*, P. sylvestris, Quercus pubescens*-type, and *Cedrus*. Rare herbaceous pollen types include Asteroideae and *Cerealia*-type.

https://doi.org/10.5194/egusphere-2025-174
Preprint. Discussion started: 18 February 2025

Hygrophilous vegetation, fungi and algae

The NPPs and hygrophilous vegetation diagram is divided into four Non-Pollen Palynomorph assemblage zones (NPPAZ) according to the CONISS method (Fig. 3B, Table 1).

NPPAZ 1 (247-184 m) is characterized by two major peaks of the green algae *Botryococcus*, the presence of the golden algae Chrysophyceae, and semi-aquatic vegetation composed of Cyperaceae and *Sparganium/Typha.*

NPPAZ 2 (184-107 m) records an increase of Chrysophyceae and semi-aquatic vegetation with Cyperaceae and *Sparganium/Typha*, whereas *Botryococcus* decreases. This zone is also marked by a high percentage of Cyperaceae at the beginning and a high percentage of *Sparganium/Typha* at the end, accompanied by the presence of macroscopic charcoal or wood in the sediment. The transition to NPPAZ 3 is marked by a large peak of *Botryococcus*.

NPPAZ 3 (107-80 m) is distinguished by a significant proportion of the green algae *Pediastrum* accompanied by *Botryococcus*, a rich semi-aquatic vegetation mainly composed of *Sparganium/Typha*, and the presence of Chrysophyceae. A peak of the fungi of type HdV-200 is recorded around 100 m.

NPPAZ 4 (80-4 m) is mainly characterized by a large proportion of Chrysophyceae and well-developed semi-aquatic vegetation. However, this zone is punctuated by two peaks of *Pediastrum* (~45 m and ~10 m) and a peak of *Lemna* (~65 m). The proportion of *Botryococcus* is low, and some fungal spores are recorded (*Sordaria, Podospora*, Coniochaeta).

https://doi.org/10.5194/egusphere-2025-174
Preprint. Discussion started: 18 February 2025

Please italicise species names.

Principal component analysis

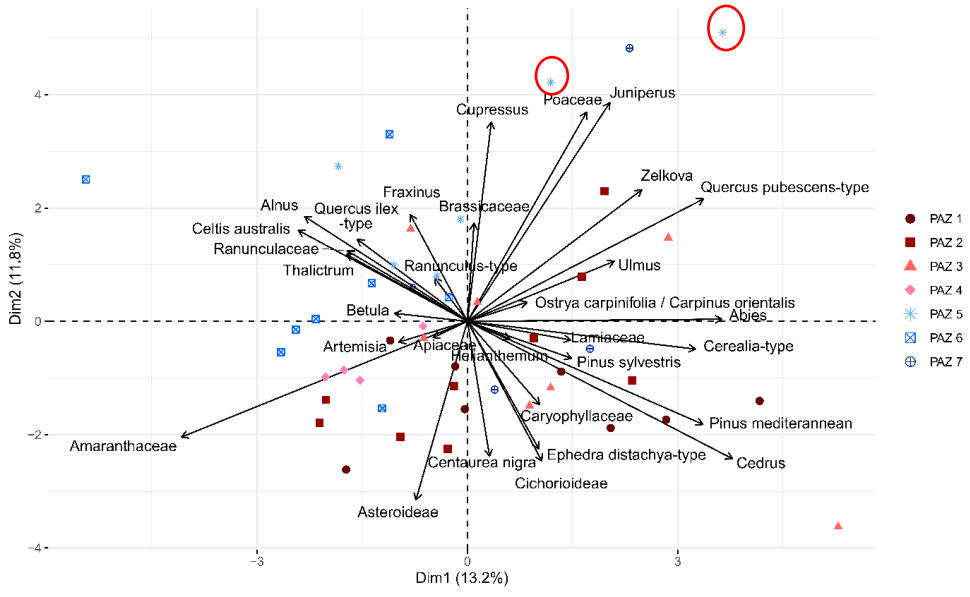

Figure 4: Principal component analysis (PCA) on selected terrestrial pollen taxa from the lacustrine succession of the Burdur Basin-fill (Türkiye). Sample map was coloured according to the PAZ (presented in Fig. 3).

Principal component analysis (PCA) was performed on selected terrestrial pollen taxa (Fig. 4) and the sample map was coloured according to the PAZ obtained with CONISS (Fig. 3A). The first two principal components (PCA 1 and PCA 2) explain 25% of the total variance (13.2% and 11.8% respectively).

PCA 1 separates the pollen samples associated with open vegetation (Amaranthaceae, *Artemisia*, Asteroideae) or local vegetation (*Fraxinus, Alnus*, Ranunculaceae) from the samples with more developed arboreal or shrub vegetation (*Quercus pubescens*-type, *Juniperus, Pinus, Cedrus, Ephedra distachya*-type). The samples from PAZ 4, 5, 6 have negative values on the first axis and are associated with open vegetation, whereas the samples from PAZ 1, 3, and 7 have positive values and are associated with more developed trees and shrubs.

PCA 2 separates the pollen samples mostly associated with steppic taxa (Amaranthaceae, Asteroideae, Cichorioideae, *Ephedra distachya*-type) from the samples associated with deciduous arboreal taxa (*Quercus pubescens*-type, *Fraxinus, Alnus, Zelkova, Ulmus, Ostrya carpinifolia/Carpinus orientalis*) and some herbaceous taxa (Poaceae, Ranunculaceae). The samples from PAZ 1, 2, and 4 have negative values on the second axis and are associated with steppic vegetation, whereas the samples from PAZ 5 have positive values and are associated with deciduous arboreal taxa.

https://doi.org/10.5194/egusphere-2025-174
Preprint. Discussion started: 18 February 2025

Large pollen grains of Poaceae

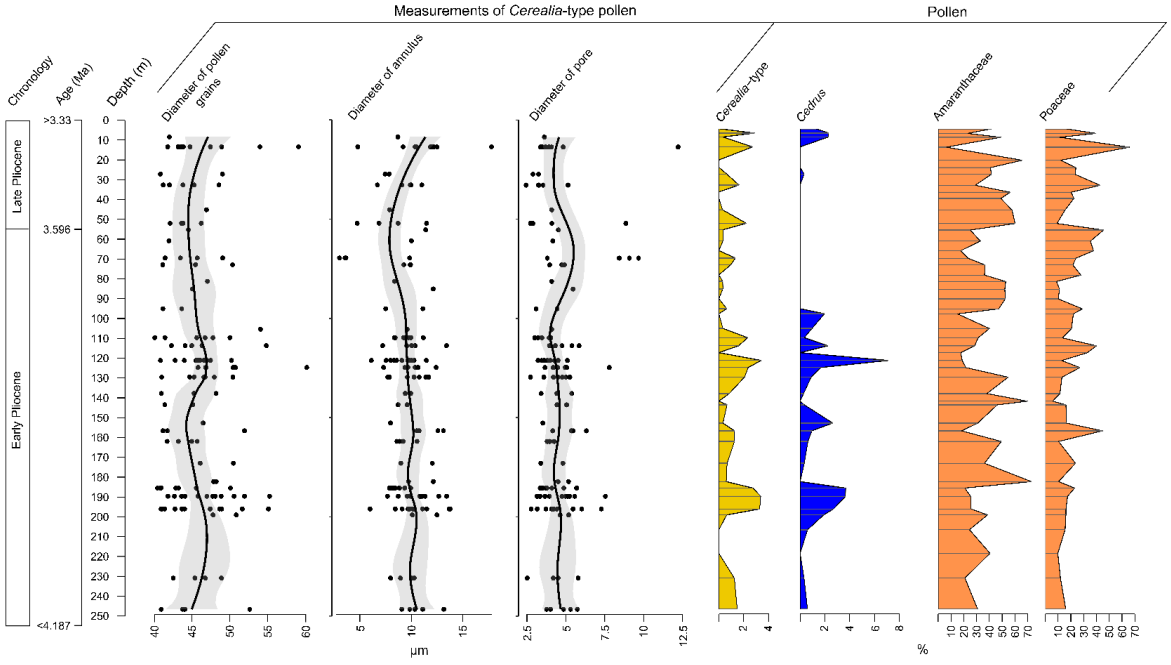

Figure 5: Measurements of diameter of pollen grains, annulus and pores of large pollen grains of Poaceae from the core BS-87 Burdur against core depth. The measurements are compared with the variation in the percentages of some of the more characteristic pollen taxa, i.e. *Cerealia*-type, *Cedrus*, Amaranthaceae and Poaceae.

A total of 133 large pollen grains of Poaceae, with a diameter larger than 40 µm, have been identified and measured along the sequence (Fig. 5). The measurements conducted on these grains reveal a mean grain diameter of 45.8 ± 3.9 µm, a mean annulus diameter of 9.7 ± 2.1 µm, and a mean pore diameter of 4.5 ± 1.4 µm. Large Poaceae grains are more abundant at the end of PAZ 1 (200-185 m), at the end of PAZ 2, and during PAZ 3 (130-100 m). The results show important variability within the same sample; however, no clear trend in size differences appears along the sequence. A large grain diameter is not necessarily associated with a large annulus or a large pore.

4.3 Pollen-inferred climate reconstructions

Results of the pollen-inferred climate reconstructions based on the five methods are shown on Figure 6. Statistical results for model performance (Supplementary Table S1) show the better R^2 and RMSE values for the BRT method. MAT, BRT and WA-PLS methods appear to be sensitive methods, unlike the RF method. CAM also appears less sensitive. However, as described above, in the CAM, the estimates are given as a climatic range, with the "most likely value" corresponding to a weighted mean. The complete climatic interval for CAM is provided in Supplementary Table S2.

The reconstructed mean annual air temperatures (MAAT) are close to modern values for WA-PLS (PAZ 1–7), slightly warmer (PAZ 1–3) and then equivalent to modern values (PAZ 4–7) for CAM, colder for BRT and

https://doi.org/10.5194/egusphere-2025-174
Preprint. Discussion started: 18 February 2025

RF (PAZ 1–7), and equivalent to modern values (PAZ 1–3) before becoming colder (PAZ 5–7) for MAT. Reconstructed mean temperature of the warmest month (MTWA) follows a similar pattern, except for MAT, which reconstructs warmer conditions compared to modern values, and BRT, which reconstructs equivalent values compared to modern conditions. Regarding the mean temperature of the coldest month (MTCO), all five methods show lower values than today, particularly the MAT, BRT, and RF approaches.

Mean annual precipitation (PANN) is close to modern values according to CAM and RF methods but significantly lower than modern values with the other three methods, especially MAT. Winter and summer precipitation, which are not reconstructed by CAM, show higher values than today, particularly with the RF method. Overall, CAM indicates few climatic variations over time, in contrast to MAT, which shows greater variability. Moreover, the temperature patterns sometimes appear reversed between CAM and the other methods.

https://doi.org/10.5194/egusphere-2025-174
Preprint. Discussion started: 18 February 2025

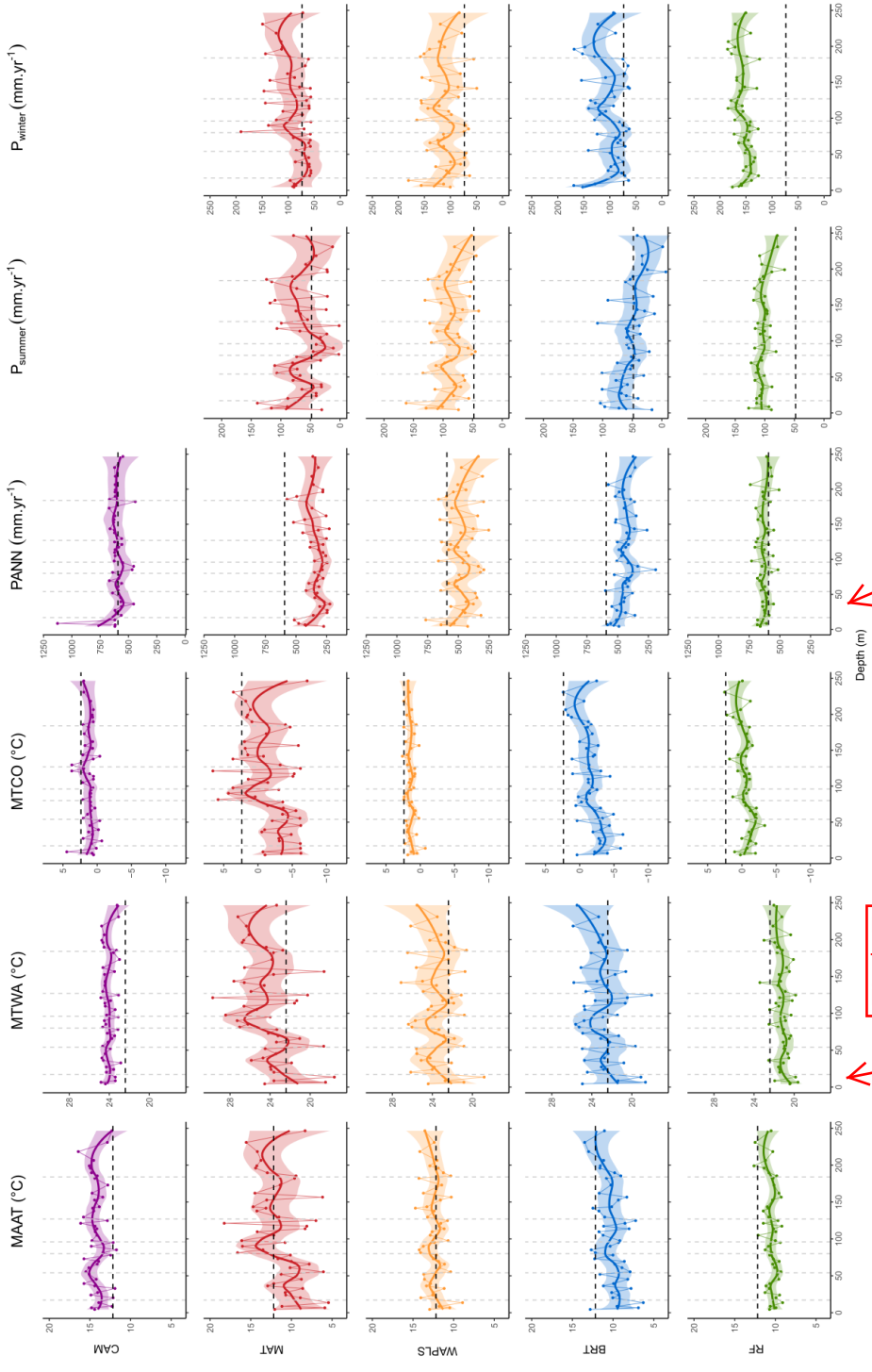

please mark the early-late Pliocene boundary, even if possible

reorganise from old to young. Or if it is, it's not clear.

https://doi.org/10.5194/egusphere-2025-174
Preprint. Discussion started: 18 February 2025

Figure 6: Lake Burdur pollen-inferred climate reconstruction based on five methods against depth: CAM (Climatic Amplitude Method), MAT (Modern Analogue Technique), WA-PLS (Weighted Averaging Partial Least Squares regression), BRT (Boosted Regression Trees) and RF (Random Forest). Large lines correspond to loess smoothed curves and shaded areas to the 95 % confidence interval. Black dashed lines correspond to modern climate values of Burdur. Grey dashed lines correspond to Pollen Assemblage Zones (Fig. 3A). MAAT: mean annual air temperature. MTWA: mean temperature of the warmest month. MTCO: mean temperature of the coldest month. PANN: mean annual precipitation. Psummer: summer precipitation. Pwinter: winter precipitation.

5. Discussion

5.1 Age-depth model

The proposed magnetostratigraphy put forward a single tie point, 3.60 Ma at 60 m depth, and brackets the top and bottom of the studied core at >3.33 and <4.19 Ma, entirely in the Pliocene with the Early-Late Pliocene transition at 60 m (Fig. 2). This would indicate a sedimentation rate higher than 51 cm/ka in the lower Pliocene section and higher than 22 cm/ka in the upper Pliocene section. Compared to the >18 cm/ka rate inferred 20 km to the north and more recently in the Burdur lake history by Özkaptan et al. (2018), the difference seems plausible based on geographic and temporal variations of sedimentation within Lake Burdur. Any other match of the 60-360 m long reverse chron within the younger sequence interpreted by Özkaptan et al. (2018) would result in unrealistically high sedimentation rate (4-5 times larger).

Our sampling interval of one meter (on average) corresponds to a time interval between samples in the 2-4 ka range. Therefore, it is not feasible to detect cyclicities of approximately 20 ka in parameters such as magnetic susceptibility.

5.2 Vegetation dynamics at Burdur and around the Mediterranean Basin during the Early-Late Pliocene transition

Wetland dynamic of Lake Burdur

During the Early Pliocene, Lake Burdur is primarily marked by two peaks of the planktonic colonial green algae *Botryococcus,* the presence of the planktonic golden-brown algae Chrysophyceae, and semi-aquatic vegetation (Cyperaceae and *Sparganium/Typha)* (Fig. 3B; NPPAZ 1). *Botryococcus* is commonly recorded in freshwater fens, temporary pools, ponds and lakes, but it can also be found in saline environments (Van Geel, 2002). *Botryococcus braunii,* the most abundant species in the Burdur sequence, can tolerate salinities up to 8% (Matthiessen and Brenner, 1996). For example, *B. braunii* has been recorded in slightly saline lakes of Australia, but they bloom only after rainfall, which reduces the lake's salinity (Wake and Hillen, 1980). *Botryococcus* develop in various ecologies including oligotrophic, mesotrophic or eutrophic conditions (Komárek and Marvan, 1992; Jankovská and Komárek, 2000). The dominance of *Botryococcus* and the absence or very sporadic occurrence of other green algae can also indicate relatively extreme environments, often characterized by very cold, clear, oligotrophic, and eventually dystrophic conditions (Jankovská and Komárek, 2000). Chrysophyceae are principally found in humic, neutral slightly acidic lakes and ponds characterized by oligotrophic conditions and less frequently by meso-eutrophic conditions (Kristiansen and Škaloud, 2017; Smol, 1988; Tolotti et al., 2003). In the Burdur record, the poorly development of semi-aquatic vegetation, the presence of the algae *Botryococcus* and Chrysophyceae and the absence of other green algae suggest oligotrophic conditions. In NPPAZ 2 (Fig. 3B), the sequence is characterized by a slight increase in Chrysophyceae and semi-aquatic vegetation with Cyperaceae and

https://doi.org/10.5194/egusphere-2025-174
Preprint. Discussion started: 18 February 2025

Sparganium/Typha, whereas *Botryococcus* decreases. The limited development of semi-aquatic vegetation and the presence of Chrysophyceae algae suggest oligotrophic or mesotrophic conditions.

The end of the Early Pliocene and the beginning of the Late Pliocene is characterized by the alternance between different trophic conditions (Fig. 3B; NPPAZ 3 and 4). Three periods (~110-80 m, ~55-30 m, ~10 m) are marked by the presence of the green algae *Pediastrum* accompanied by *Botryococcus*, semi-aquatic vegetation (Cyperaceae, *Sparganium/Typha*) and the presence of Chrysophyceae algae. The planktonic colonial green algae *Pediastrum* is recorded in freshwater fens, temporary pools, ponds and lakes, however it can also live in saline environments (Komárek and Jankovská, 2001; Van Geel, 2002). *Pediatrum boryanum,* the most abundant species in the Burdur sequence, tolerates salinities up to 8% (Matthiessen and Brenner, 1996). *Pediastrum* is particularly common in hard-water eutrophic lakes (Van Geel, 2002). The association between semi-aquatic vegetation, green algae (*Botryococcus* and *Pediastrum*) and Chrysophyceae suggest mesotrophic or eutrophic conditions. On the contrary, two periods (~80-55 m, ~30-15 m) are characterized by a large dominance of Chrysophyceae, the presence of semi-aquatic vegetation (Cyperaceae, *Sparganium/Typha)* and a peak of *Lemna* at ~65 m. *Lemna* is a free-floating aquatic plant, and the increase in plant biomass, such as *Lemna*, over a short time contributes to lake eutrophication (Gostyńska et al., 2022). The association between Chrysophyceae algae and semi-aquatic and aquatic vegetation suggests mesotrophic conditions at between 80 and 55 m and oligotrophic or mesotrophic conditions between 30 and 15 m.

Steppe vegetation in Southwestern Anatolia

The Early Pliocene is dominated by steppe taxa, including *Artemisia,* Amaranthaceae and Poaceae, and an arboreal signal with *Quercus pubescens*-type and *Pinus* mediterranean-type (Fig. 3A; PAZ 1). The percentage of *Artemisia* is particularly important at the beginning of the sequence of Burdur. *Artemisia* is a well-documented taxon in semi-desert steppe environments (Robles et al., 2022; Zhao et al., 2022). When the pollen percentage of *Artemisia* is higher than 30%, the *Artemisia* cover in the local vegetation is at least greater than 5% (Zhao et al., 2022). Today, steppe vegetation dominated by *Artemisia* is primarily recorded in Syria (El-Moslimany, 1990), Jordan (Davies and Fall, 2001), Iran (Djamali et al., 2009), China (e.g. Zhao and Herzschuh, 2009; Xu et al., 2009; Li et al., 2011; Zhang et al., 2018; Zhao et al., 2022) and Mongolia (Ma et al., 2008). The arboreal pollen taxa are mainly *Quercus pubescens*-type and *Pinus* mediterranean-type, representing 6% and 12%, respectively, of the Burdur signal. These arboreal taxa are high pollen producers and are adapted for wind dispersal (Connor et al., 2004), they can be transported over long distances, even in the presence of significant topographic barriers (Ramezani, 2013; Robles et al., 2022). Moreover, in such large sedimentation basins, pollen grains of Pinaceae are generally transported by rivers and may be dispersed from higher elevations (Suc et al., 2018). *Quercus pubescens* pollen could represent up to 15%, even if no trees were present in the catchment (Robles et al., 2022). In the Burdur record, the pollen signal of *Quercus pubescens*-type and *Pinus* mediterranean-type can be interpreted as a regional signal. At the end of the period *Cedrus*, along with large Poaceae pollen grains, is recorded. *Cedrus* is observed in a wide variety of environment, from semi-arid to humid areas, but it is particularly adapted to cool to cold climatic conditions (Magri and Parra, 2002; Quézel and Médail, 2003; Jiménez-Moreno et al., 2020; Xiao et al., 2022). This taxon has good wind dispersal and is currently found at mid to high elevations (~1500-2500 m.a.s.l.) in the Mediterranean mountains of North Africa (Rif and Atlas Mountains) and in the Middle East (Türkiye, Syria, Lebanon) (Quézel and Médail, 2003). We suggest that *Cedrus* represents a regional signal originating from the mountains of Southwestern Anatolia.

https://doi.org/10.5194/egusphere-2025-174
Preprint. Discussion started: 18 February 2025

In PAZ 2 (Fig. 3A) the vegetation is also characterized by steppe taxa, including Amaranthaceae, *Artemisia*, Poaceae and *Ephedra distachya*-type, while the arboreal taxa remain stable. The percentage of Amaranthaceae in the Burdur sequence is particularly high, reaching up to 46%. Amaranthaceae is common in semi-arid regions, representing 30% to 80% of the pollen signal (Connor et al., 2004; Robles et al., 2022). Today, desert or steppe-desert vegetation, dominated by Amaranthaceae, is primarily recorded in Iraq (El-Moslimany, 1990), Saudi Arabia (El-Moslimany, 1990), Armenia (Robles et al., 2022), China (e.g. Xu et al., 2009; Zhao and Herzschuh, 2009; Wei et al., 2011; Zheng et al., 2014; Wei and Zhao, 2016) and Mongolia (Ma et al., 2008; Zheng et al., 2014). *Ephedra* is a shrub characteristic of arid and semi-arid desert (Herzschuh et al., 2004; Zheng et al., 2014). *Ephedra distachya*-type is more particularly associated with semi-desert conditions, mainly in mountainous environments (Herzschuh et al., 2004; Zhao and Herzschuh, 2009). The dominance of Amaranthaceae and the presence of *Ephedra distachya*-type suggest drier conditions than for the previous period during the Early Pliocene. As previously mentioned, the pollen signals of *Quercus pubescens*-type and *Pinus* mediterranean-type can be interpreted as a regional indicators in the Burdur region.

In PAZ 3 (Fig. 3A) the steppe vegetation is dominated by Poaceae, Amaranthaceae, *Artemisia,* is recorded and the arboreal pollen taxa increase slightly due to a rise in *Pinus* mediterranean-type and *Cedrus*. During this period, pollen of Poaceae and Amaranthaceae dominate the pollen signal with similar percentages. In general, Poaceae is under-represented in pollen assemblages and often constitutes about a quarter of the vegetation in steppes of Central Asia (Ge et al., 2017). However, in the Caucasus, several studies have indicated that Poaceae pollen is strongly associated with the vegetation (Connor et al., 2004; Robles et al., 2022). Conversely, Amaranthaceae pollen is over-represented due to wind transport dispersal, long-distance transport capacity and high pollen production (Li et al., 2005; Zheng et al., 2008). The steppe vegetation around Lake Burdur was probably dominated by Poaceae. Today, steppe vegetation dominated by Poaceae is recorded in Georgia (Connor et al., 2004), Armenia (Robles et al., 2022), Iran (Djamali et al., 2009) and China (Zhao et al., 2009). This vegetation type is often present at high elevations, as in Armenia, where Poaceae pollen can dominate the signal from 1900 m and represents around 30% of the pollen record (Robles et al., 2022). As previously, the pollen signal of *Quercus pubescens*-type, *Pinus* mediterranean-type and *Cedrus* can be interpreted as a regional signal, with *Cedrus* originating from mountainous environments. The increase in Poaceae and arboreal pollen taxa suggests wetter conditions.

During the next period, steppe vegetation includes Amaranthaceae, *Artemisia* and Poaceae, while arboreal pollen decreases drastically (Fig. 3A; PAZ 4). The pollen signal is largely dominated by Amaranthaceae, with the percentage exceeding 50%. The dominance of Amaranthaceae and the decline in arboreal pollen taxa can be attributed to drier conditions than previously.

The last period of the Early Pliocene is also characterized by steppe vegetation including Poaceae, Amaranthaceae, *Artemisia,* (Fig. 3A; PAZ 5). The arboreal pollen taxa increase significantly with the presence of deciduous (*Quercus pubescens*-type, *Zelkova, Fraxinus*) and coniferous (*Pinus* mediterranean-type*, P. sylvestris, Juniperus, Abies*) trees. The increase of Poaceae and arboreal pollen taxa can suggest more humid conditions.

The Late Pliocene (Piacenzian Stage) is primarily characterized by steppe vegetation including Amaranthaceae, Poaceae, *Artemisia*, whereas arboreal pollen taxa decrease significantly (Fig. 3A; PAZ 6). The dominance of Amaranthaceae, with a percentage exceeding 50%, and the decline in arboreal pollen taxa can be attributed to drier conditions during the Late Pliocene, similar to the end of the Early Pliocene (PAZ 4).

https://doi.org/10.5194/egusphere-2025-174
Preprint. Discussion started: 18 February 2025

Finally, the last period is characterized by steppe vegetation with Poaceae, Amaranthaceae and *Artemisia* and (Fig. 3A; PAZ 7). Arboreal pollen taxa increase again and include *Pinus* mediterranean-type, *P. sylvestris, Quercus pubescens*-type, and *Cedrus*. The percentage of pollen of Poaceae, exceeding 30%, suggests a steppe vegetation dominated by Poaceae. Furthermore, the dominance of Poaceae and the increase in arboreal pollen taxa suggests more humid conditions.

In summary, the recorded vegetation of Southwestern Anatolia predominantly shows steppe vegetation during the Early-Late Pliocene transition, a similar vegetation pattern has been found for the Pleistocene at Lake Acıgöl, although *Pinus* is more present at certain times (Andrieu-Ponel et al., 2021).

Vegetation changes around the Mediterranean Basin

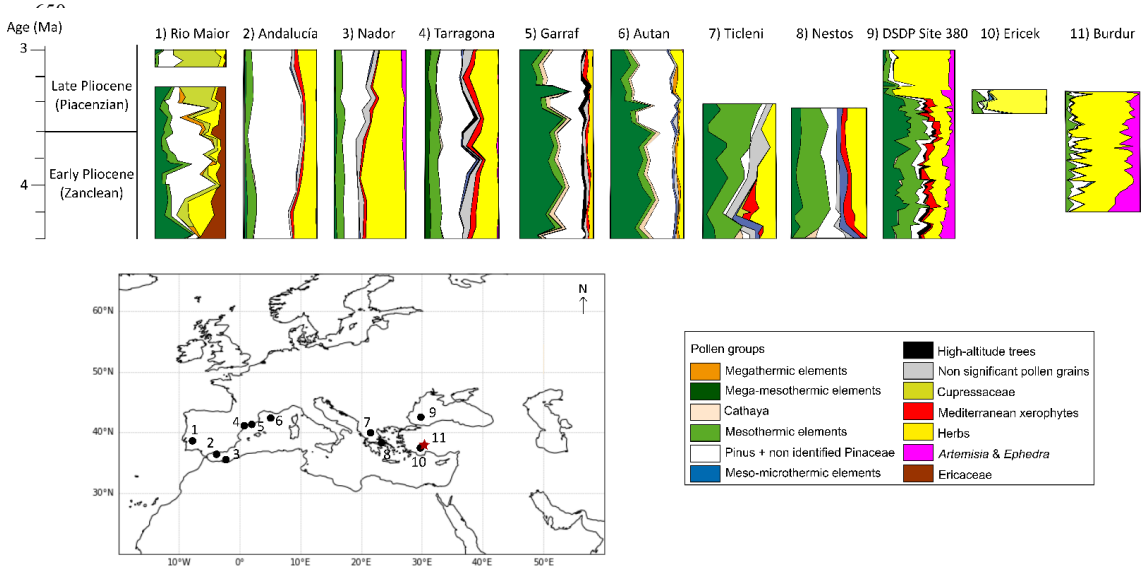

Figure 7: Vegetation reconstructions around the Mediterranean Basin for the Early-Late Pliocene transition for selected paleoenvironmental studies: 1) Rio Maior F16 (Diniz, 1984), 2) Andalucía G1 (Suc et al., 1995), 3) Nador (Feddi et al., 2011), 4) Tarragona E2 (Bessais and Cravatte, 1988), 5) Garraf 1 (Suc and Cravatte, 1982), 6) Autan 1 (Cravatte and Suc, 1981), 7) Ticleni 1 (Jiménez-Moreno et al., 2007), 8) Nestos 2 (Jiménez-Moreno et al., 2007), 9) DSDP site 380 (Popescu, 2006), 10) Ericek (Jiménez-Moreno et al., 2015) and 11) Burdur (this study) presented in percentages. The description of ecological classification of pollen taxa is presented in Supplementary Table S3.

The pollen records available to document the Early-Late Pliocene transition are mainly located in the Western Mediterranean Basin (Fig. 7; e.g. Jiménez-Moreno et al., 2010; Suc et al., 2018) or in the Balkans (Jiménez-Moreno et al., 2007) whereas in the central Mediterranean, continuous records covering this time period are lacking (Combourieu-Nebout et al., 2015). In the Eastern Mediterranean, only the pollen records from the Black Sea (DSDP Site 180; Popescu, 2006) and in southwestern Tükyie (Jiménez-Moreno et al., 2015) cover this time period.

During the final part of the Early Pliocene (Zanclean period, 4–3.6 Ma), a contrasting pattern is recorded around the Mediterranean Basin, with southern records (Andalucía, Nador, Tarragona, Burdur) characterized by open vegetation and northern records (Autan, Garraf, Nestos, Ticleni, DSDP Site 380) characterized by deciduous

https://doi.org/10.5194/egusphere-2025-174
Preprint. Discussion started: 18 February 2025

forests (Cravatte and Suc, 1981; Suc and Cravatte, 1982; Bessais and Cravatte, 1988; Suc et al., 1995; Jiménez-Moreno et al., 2007; Popescu et al., 2010; Feddi et al., 2011). However, the latitudinal limit differs depending on the longitudinal location and the pollen assemblages can be site-dependent according to the geographical context (e.g. Tarragona and Garraf). Specifically, on the Atlantic side of the Iberian Peninsula, the site of Rio Maior (Diniz, 1984) is characterized by the dominance of mega-mesothermic trees and Ericaceae. This site stands out from other records due to the high representation of Ericaceae, a characteristic element of the current vegetation of the Atlantic coast. In the south of the Iberian Peninsula, the sites of Andalucía (Suc et al., 1995) and Nador (Feddi et al., 2011) include a large proportion of herbaceous taxa and *Pinus*. Early Pliocene vegetation records are close to modern open sub desertic environments in the Southwestern Mediterranean (Suc et al., 1995). In Northwestern Spain, the site of Tarragona (Bessais and Cravatte, 1988) also records a large proportion of herbaceous pollen taxa and *Pinus*. Conversely, the site of Garraf (Suc and Cravatte, 1982) in Northwestern Spain and the site of Autan (Cravatte and Suc, 1981) in the South of France are characterized by mega-mesothermic trees. In the Balkans, the sites of Nestos and Ticleni show a large proportion of mesothermic trees and the presence of megathermic taxa (Jiménez-Moreno et al., 2007 and references therein). In the eastern part of the Mediterranean Basin, the record from the Black Sea (DSDP Site 380) shows a high proportion of abundant mega-mesothermic and mesothermic elements, including Cupressaceae and *Cathaya* (Popescu et al., 2010). The Pliocene period corresponds to extensive forest environments on the Black Sea coastal plains. In contrast, the Burdur site in Southwestern Türkiye reveals steppe vegetation dominated by Amaranthaceae, *Artemisia* and Poaceae. Our record is distinctive due to the very low presence of arboreal taxa and the absence of relict taxa. Several studies suggested the presence of *Artemisia* steppes in Anatolia during this period (Popescu, 2006; Suc et al., 2018). However, at Burdur, the steppe was dominated either by *Artemisia*, Amaranthaceae, or Poaceae, depending on the period. In Central Asia, on the Tibetan Plateau, semi-desert and desert environments are well represented, with vegetation including Amaranthaceae, *Artemisia*, Poaceae and Cyperaceae (Koutsodendris et al., 2019; Schwarz et al., 2023).

At the transition between the Early and Late Pliocene (Piacenzian period, 3.6–3.4 Ma), strong vegetation changes are recorded around the Mediterranean Basin, including an increase in deciduous trees (Fig. 7). However, a contrasting pattern is identified between the western regions (Rio Maior, Andalucía, Nador, Tarragona, Garraf) dominated by *Pinus*, and the eastern regions (DSDP Site 180, Ericek, Burdur) characterized by open vegetation (Cravatte and Suc, 1981; Suc and Cravatte, 1982; Bessais and Cravatte, 1988; Diniz, 1984; Suc et al., 1995; Popescu et al., 2010; Feddi et al., 2011; Jiménez-Moreno et al., 2015). In the Western Mediterranean region, the sites of Rio Maior, Garraf and Autan record a significant decrease in mega-mesothermic elements, accompanied by a marked increase of *Pinus* (Suc and Cravatte, 1982; Cravatte and Suc, 1981; Diniz, 1984). In the south of Spain (Andalucía), and Northern Morocco (Nador) herbaceous taxa are still abundant, but the open formations are marked by the development of *Artemisia* and *Ephedra* steppes. *Pinus* increases significantly at Nador, while high altitude trees such as *Cedrus*, *Tsuga* or *Cathaya* appear alongside Mediterranean xerophytes (*Olea*, *Quercus* type *ilex-coccifera*) in Andalucía (Suc et al., 1995; Feddi et al., 2011). In the Eastern Mediterranean region, arboreal pollen taxa decline in the record, notably in the Black Sea (DSDP Site 380; Popescu, 2006) with a less abrupt decrease in Southwestern Anatolia (Burdur, this study). In contrast, herbaceous taxa dominated the pollen records. Open vegetation with Poaceae is also recorded at the Ericek site in Southwestern Anatolia, where the percentage of relict taxa is very low (Jiménez-Moreno et al., 2015). In Burdur, steppe vegetation is also observed, with dominance of either Poaceae or Amaranthaceae; however, no relict taxa were recorded. In Central Asia, desert and

https://doi.org/10.5194/egusphere-2025-174
Preprint. Discussion started: 18 February 2025

semi-desert vegetation is dominated by Amaranthaceae, *Artemisia*, Poaceae, Cyperaceae, and Ephedraceae (Koutsodendris et al., 2019; Schwarz et al., 2023). Since the Late Pliocene, Central Asia has recorded an increase of Amaranthaceae and an alternation between desert vegetation, dominated by Amaranthaceae, and steppe vegetation, dominated by *Artemisia* with increasing Poaceae (Schwarz et al., 2023). A similar alternation is observed in Burdur, with dominance shifting between Amaranthaceae and Poaceae. This difference, with *Artemisia* dominance in Central Asia and Poaceae dominance in Southwestern Anatolia, is likely related to variations in precipitation between the two regions.

5.3 Climate changes around the Mediterranean Basin during the Early-Late Pliocene transition

Climate changes in Southwestern Anatolia

Pollen-inferred climate changes using a multi-method approach have, for the first time, been reconstructed for a period before the Quaternary. CAM is typically used for the Neogene period, when no pollen assemblage analogs exist in modern pollen floras (Fauquette et al., 1998a, b). However, the Burdur vegetation, characterized by steppe vegetation and the absence of relict taxa (Fig. 3A), allows for testing other methods commonly used to reconstruct the climate of more recent time periods (MAT, WA-PLS, etc.). Climate reconstructions of Burdur show similar trends across the different methods used here, except for CAM, particularly during the Late Pliocene (Fig. 6). The reconstructed climatic interval for CAM may be broader (Supplementary Table S2) as it is often the case in open-vegetation environments (Fauquette et al., 1999). The absence of relict taxa and the wide climatic range of taxa like Poaceae prevent full constraint of the climate reconstruction amplitude. The RF method appears to overestimate reconstructed seasonal precipitation values compared to other methods (Fig. 6). This is likely due to the relative contribution of taxa with the highest percentages, which are low-pollen taxa with limited ecological importance in the study area (Salonen et al., 2019). The most effective methods, with the highest R^2 and lowest RMSE values for all climatic parameters, are the BRT and MAT methods (Supplementary Table S1). For MAT, spatial autocorrelation is low (Moran's I<0.19, p-value<0.01). For BRT, the "boosting" process enhances model performance, making it particularly effective for microfossil datasets (Salonen et al., 2019; Chevalier et al., 2020). Based on the statistical performance of the methods and to allow comparisons with previous pollen-inferred climate reconstructions in the Mediterranean region (Fauquette et al., 2007), climate reconstructions based on MAT, BRT, and CAM are used for the discussion section.

Mediterranean climate conditions, with hot, dry summers and cool, wet winters are reconstructed from the Burdur pollen assemblages (Fig. 6). Climate reconstructions primarily indicate a climatic optimum in terms of precipitation and temperature recorded by the different methods (PAZ 1 and 2). This period is characterized by the highest percentages of arboreal pollen taxa in the Burdur records and oligotrophic to mesotrophic conditions in the lake (Fig. 3). Subsequently, climate reconstructions show an alternation between cool, wet conditions (PAZ 3, 5, and 7) and warm, dry conditions (PAZ 4 and 6), particularly with the MAT. However, the climatic oscillations reconstructed with the MAT appear very large for this time period. Several studies (Suc, 1984; Suc et al., 2018), suggest that the Mediterranean Basin experienced the establishment of a Mediterranean climate during the Pliocene, characterized by a seasonal rhythm with summer droughts and cool, wet winters. At Burdur, Mediterranean climate conditions are also evident during the Pliocene.

https://doi.org/10.5194/egusphere-2025-174
Preprint. Discussion started: 18 February 2025

Climate changes around the Mediterranean Basin

Around the Mediterranean Basin, other pollen-inferred climate reconstructions have been conducted for the western region using CAM (Fauquette et al., 1999, 2007; Jiménez-Moreno et al., 2010; Feddi et al., 2011). During the final part of the Early Pliocene (Zanclean period, 4–3.6 Ma), pollen-inferred climate reconstructions for the Western Mediterranean (Rio Maior, Andalucía, Nador, Tarragona, and Garraf) indicated warmer than present conditions (Fauquette et al., 1999, 2007) similar to the results for Burdur using CAM. However, this trend is not reflected by the other methods (Fig. 6). Sea surface temperature (SST) reconstructions based on alkenones from the island of Cyprus also reveal higher values compared to modern conditions (Athanasiou et al., 2017). Although a cooling event is detected at ~3.91 Ma, corresponding to the global MIS Gi16 (Athanasiou et al., 2017). Temperature reconstructions from the Teruel site in Spain, based on lacustrine $\delta^{18}O_c$ (Ezquerro et al., 2022) and from sites in Cyprus and Italy, based on planktonic $\delta^{18}O$ (Colleoni et al., 2012 and references therein) also indicate warm conditions. The climate around the Mediterranean Sea was primarily influenced by the 23 kyr precession cycle and an intensification of African monsoonal activity (Colleoni et al., 2012; Athanasiou et al., 2017). Precipitation close to modern values has been reconstructed for Andalucía and Nador, while more humid conditions are recorded for Tarragona and Garraf (Fauquette et al., 1999, 2007). In the Eastern Mediterranean, pollen-inferred climate reconstructions of Burdur show precipitation similar to modern conditions (Fig.7). As for vegetation, and as previously highlighted by Fauquette et al. (2007) and Jiménez-Moreno (2010), pollen-inferred reconstructions reveal a north-south precipitation pattern, with wetter conditions in the Northern Mediterranean compared to the south. However, the number of sites is limited, and additional precipitation reconstructions are needed for the Eastern Mediterranean.

During the Late Pliocene (Piacenzian period, 3.6–3.4 Ma), warmer than present conditions have been reconstructed for the Western Mediterranean (Rio Maior, Andalucía, Nador, Tarragona, and Garraf) by Fauquette et al. (1999, 2007), similar to the results for Burdur with CAM, whereas lower values are recorded with other methods (Fig. 6). SSTs based on alkenones show warmer conditions (~4°C higher than modern values) in the islands of Cyprus (Athanasiou et al., 2017) and Italy (Herbert et al., 2015; Plancq et al., 2015). However, the site from Cyprus shows a decrease in temperature compared to the Early Pliocene (Athanasiou et al., 2017). The SST reconstruction reveals the presence of two cooling events at 3.58 Ma and 3.34–3.31 Ma, corresponding to MIS MG12 and MIS M2 (Plancq et al., 2015; Athanasiou et al., 2017). The temperature reconstruction for the Teruel site in Spain, based on lacustrine $\delta^{18}O_c$, shows a significant decrease in values from 3.6 to 3 Ma (Ezquerro et al., 2022). In the islands of Cyprus and in Italy, $\delta^{18}O$ planktonic records indicate a temperature decrease during the Late Pliocene (Colleoni et al., 2012 and references therein). Climate changes in the Mediterranean Sea during the Late Pliocene were dominated by cycles of the 23 kyr precession, accompanied by an intensification of African monsoonal activity (Herbert et al., 2015; Athanasiou et al., 2017). Obliquity-related rhythms significantly influenced SST after 2.8 Ma and dominated the signal after 2.51 Ma (Herbert et al., 2015). In terms of precipitation, a general increase is recorded in the Western Mediterranean for the sites of Rio Maior, Nador, and Garraf. However, some sites, including Andalucía and Tarragona, show little change, with conditions close to modern values. In the Eastern Mediterranean, the site of Burdur shows values close to modern levels, except for PANN reconstructed by MAT, which indicates lower values than today (Fig. 6). Precipitation estimates for the Teruel site in Spain, based on lacustrine $\delta^{18}O_c$, suggest more humid conditions, particularly between 3.6 and 3 Ma (Ezquerro et al., 2022). For the sites on the islands of Cyprus and in Italy, $\delta^{18}O$ planktonic records show a more progressive

https://doi.org/10.5194/egusphere-2025-174
Preprint. Discussion started: 18 February 2025

decrease in precipitation during the Late Pliocene (Colleoni et al., 2012 and references therein). In Central Asia, dry conditions are suggested from 3.8 Ma, likely linked to a weakening of the East Asian Monsoon (Schwarz et al., 2023). The Late Pliocene appears to be marked by more humid conditions in the Western Mediterranean, whereas Tükyie and Central Asia show more arid conditions. A weak AMOC is identified in Europe from 3.8 to 3 Ma, leading to cooler and wetter conditions primarily in the Northwestern Mediterranean (Karas et al., 2017; Ezquerro et al., 2022).

Moreover, the simulations of GCMs performed as part of the the 2nd Pliocene Model Intercomparison Project (PlioMIP2), spanning from 3.264 to 3.025 Ma, indicate warmer conditions compared to pre-industrial values around the Mediterranean Basin (Haywood et al., 2020). In terms of precipitation, a latitudinally contrasted pattern is reconstructed, with wetter conditions in Northern Europe and drier conditions in the south (Fig. 8). More specifically, Spain, Greece, and Türkyie exhibit conditions similar to today or slightly more arid (Haywood et al., 2020; Feng et al., 2022). Climate reconstructions based on data show similar conditions in Southern Spain and Western Türkiye as in the model. However, in Western and Northern Spain, Southern France, and Italy, wetter conditions are recorded by the data. In the Eastern Mediterranean, the data indicate wetter conditions except in Western Türkiye and the western and eastern coasts of the Black Sea.

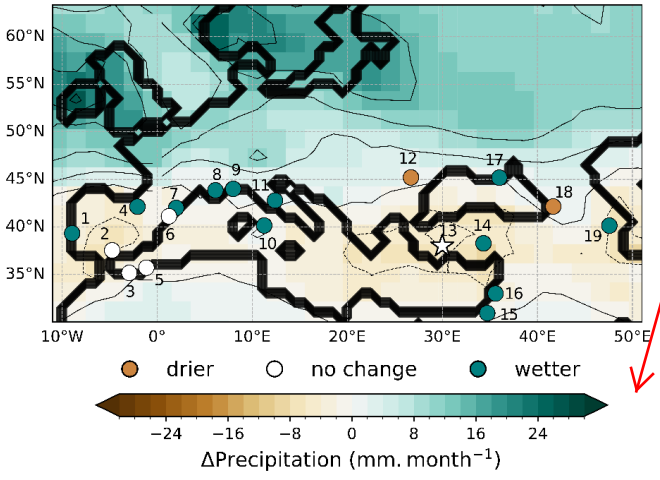

Please, could you please add data for Burdur area in the Supplementary file in mm.month-1 scale. In order to see the data showing that there is no change in the amount of precipitation.

Figure 8: Model-Data comparison from 3.264 to 3.025 Ma. Precipitation anomalies and comparison between PlioMIP2 and selected data around the Mediterranean Basin: 1) Rio Maior F16 (Fauquette et al., 1999), 2) Andalucía G1 (Fauquette et al., 1999), 3) Nador (Fauquette et al., 1999), 4) Villarroya (Muñoz et al., 2002; Anadón et al., 2008) (Munoz et al., 2002; Anadon et al., 2008), 5) Habibas 1 (Fauquette et al., 1999), 6) Tarragona E2 (Fauquette et al., 1999), 7) Garraf (Fauquette et al., 2007), 8) Puimoisson (Blavoux et al., 1999), 9) St Isidore (Fauquette et al., 2007), 10) ODP 653 (Bertoldi et al., 1989), 11) Tiberino Basin (Basilici, 1997), 12) Dacian Basin (Van Baak et al., 2015), 13) Burdur (this study), 14) Ihlara-Selime (Gürel and Yıldız, 2007), 15) Ashalim Cave (Vaks et al., 2013), 16) Hula Basin (Horowitz, 1989), 17) Kerch Peninsula (Salzmann et al., 2008), 18) Colchis (Shatilova, 1986), 19) Azerbaijan (Salzmann et al., 2008). Data originating from Feng et al., 2022.

5.4 Characterization of large Poaceae pollen grains and comparison with other pollen records

The large pollen grains of Poaceae are recorded in the Burdur record, but the percentages are lower than at Acıgöl (Andrieu-Ponel et al., 2021), not exceeding 3.5% (Fig. 5) while at Acıgöl the percentages reach 7%. The

https://doi.org/10.5194/egusphere-2025-174
Preprint. Discussion started: 18 February 2025

morphological characteristics of large Poaceae grains from Burdur are similar to those of domesticated cereals in recent periods. However, a clear distinction between pollen of domesticated and wild Poaceae from Burdur is not possible based solely on morphological characteristics. Modern pollen identification keys establish the boundary between wild and domesticated Poaceae pollen based on the following measurements: pollen grain diameter between 37 µm and 47 µm, annulus diameter between 8 µm and 11 µm, and pore diameter between 3 µm and 4 µm (Andersen, 1979; Beug, 2004; Tweddle et al., 2005; Joly et al., 2007). The measurements taken from large Poaceae pollen grains at Burdur exceed these limits, even when considering two criteria, as suggested by Andersen (1979) and Joly et al. (2007). The difficulty in distinguishing between wild and domesticated Poaceae pollen is further compounded by the presence of the genus *Lygeum* in some Mediterranean Pliocene records (Bessais and Cravatte, 1988). *Lygeum spartum* is characteristic of semi-arid Mediterranean areas, and its pollen is noted for its elongated shape, large grain diameter (~80 µm), and prominent annulus (Reille, 1998). However, *Lygeum* pollen has not been identified in the Burdur sequence, and no large Poaceae pollen grains displayed an elongated shape resembling that of *Lygeum*.

High percentages of large pollen grains of Poaceae) are positively correlated with *Cedrus* and negatively correlated with Amaranthaceae (Fig. 5; Supplementary Figure S2). *Cedrus* is particularly adapted to cool to cold climatic conditions (Magri and Parra, 2002; Quézel and Médail, 2003; Jiménez-Moreno et al., 2020; Xiao et al., 2022), while Amaranthaceae is commonly found in desert environments (e.g. Zheng et al., 2014; Robles et al., 2022). Andrieu-Ponel et al. (2021) proposed several hypotheses to explain the presence of proto-cereal pollen, including the impact of large herbivore herds on steppe ecosystems (Spengler et al., 2021; Malhi et al., 2022) and the emergence of polyploidy in some Poaceae species under drought conditions (Manzaneda et al., 2012). In contrast to the results obtained at Acıgöl, Burdur shows a low proportion of coprophilous spores, and the vegetation does not suggest drought conditions during periods when large Poaceae pollen are more abundant (Figs. 3, 6). However, these two sites do not cover the same time period and are associated with different environmental and climatic contexts. Additionally, a study focusing on the size of large Poaceae pollen grains is needed to better understand the relationship between their size and climate changes.

6. Conclusion

Based on the new Burdur pollen sequence, this study provides valuable insights into the environmental changes (vegetation and climate) during the Early–Late Pliocene transition in the Eastern Mediterranean, a poorly documented time period and region. The Burdur core records an open vegetation alternating between steppe grasslands with deciduous *Quercus* and steppes dominated by Amaranthaceae. The lacustrine ecosystem was characterized by semi-aquatic vegetation and freshwater algae, exhibiting alternating oligotrophic and eutrophic conditions. While large Poaceae pollen grains are recorded, their percentages are relatively low compared to those from Lake Acıgöl, which covers a more recent period. Additionally, the morphological measurements do not allow for differentiation between wild and domesticated Poaceae. Climate reconstructions indicate a climatic optimum of precipitation and temperature before the Early–Late Pliocene transition, followed by an alternation between relatively cool, wet conditions and warm, dry conditions after the Early–Late Pliocene transition. However, the amplitude of the reconstructed oscillations appears to be too large for this time period.

https://doi.org/10.5194/egusphere-2025-174
Preprint. Discussion started: 18 February 2025

A contrasting pattern characterizes the Early Pliocene around the Mediterranean basin, with southern records showing open vegetation and northern or central records dominated by deciduous forests. Climate reconstructions based on various proxies indicate warmer conditions compared to modern values, with a noticeable north-south gradient, where the Northern Mediterranean experienced wetter conditions than the south. In the Late Pliocene, an increase in deciduous trees is recorded, and a contrasting pattern emerges between the western regions, dominated by *Pinus*, and the eastern regions, characterized by open vegetation. The Late Pliocene appears colder, marked by more humid conditions in the Western Mediterranean, while Türkyie and Central Asia experienced more arid conditions. A weak AMOC is identified in Europe from 3.8 to 3 Ma, leading to cooler and wetter conditions primarily in the Northwestern Mediterranean.

Author contribution

MR: Laboratory work (pollen, NPPs), Formal analysis (climate reconstruction), Writing draft manuscript, Review, Funding acquisition. VA: Conceptualization, Core sampling, Review, Funding acquisition. PR: Laboratory work (paleomagnetism), Review. SF: Formal analysis (climate reconstruction for CAM method), Review. OPe: Review. FD: Laboratory work (paleomagnetism), Review. OPa: Core sampling. EC: Laboratory work (pollen extraction). BG: Review. MCA: Laboratory work (magnetic susceptibility), Review.

Declaration of competing interest

At least one of the (co-)authors (O. Peyron) is a member of the editorial board of Climate of the Past but the authors declare that they have no known competing financial interests or personal relationships that could have appeared to influence the work reported in this paper.

Funding

This study was financially supported by the ANR FOOD-Re project (PI: V. Andrieu). The geological fieldwork was funded by the Scientific and Technological Research Council of Türkiye (TÜBİTAK) under the research grant ÇAYDAG 105Y280. Conference funding was provided by the Association des Palynologues de Langue Française (APLF).

Acknowledgements

The studied core was collected as part of the Huntite Exploration Project in the Lake District, conducted by the Mineral Research and Exploration Directorate of Türkiye (MTA), under Project Number 2018-32-13-21. The authors would like to thank Gonzalo Jiménez-Moreno for providing access to the pollen data of Ericek. This is an ISEM contribution n°2025-XXX.

References

Alçiçek, M. C., Mayda, S., and Titov, V. V.: Lower Pleistocene stratigraphy of the Burdur Basin of SW Anatolia, Comptes Rendus Palevol, 12, 1–11, https://doi.org/10.1016/j.crpv.2012.09.005, 2013.

Alçiçek, M. C., Mayda, S., ten Veen, J. H., Boulton, S. J., Neubauer, T. A., Alçiçek, H., Tesakov, A. S., Saraç, G., Hakyemez, H. Y., Göktaş, F., Murray, A. M., Titov, V. V., Jiménez-Moreno, G., Büyükmeriç, Y., Wesselingh, F. P., Bouchal, J. M., Demirel, F. A., Kaya, T. T., Halaçlar, K., Bilgin, M., and van den Hoek Ostende, L. W.: Reconciling the stratigraphy and depositional history of the Lycian orogen-top basins, SW Anatolia, Palaeobio Palaeoenv, 99, 551–570, https://doi.org/10.1007/s12549-019-00394-3, 2019.

Anadón, P., Utrilla, R., Vázquez, A., Martín-Rubio, M., Rodriguez-Lázaro, J., and Robles, F.: Paleoenvironmental evolution of the Pliocene Villarroya Lake, northern Spain, from stable isotopes and trace-element geochemistry of ostracods and molluscs, J Paleolimnol, 39, 399–419, https://doi.org/10.1007/s10933-007-9121-2, 2008.

Andersen, S. T.: Identification of wild grass and cereal pollen, Danmarks Geologiske Undersøgelse Årbog, 69-92., 1979.

https://doi.org/10.5194/egusphere-2025-174
Preprint. Discussion started: 18 February 2025

Andrieu-Ponel, V., Rochette, P., Demory, F., Alçiçek, H., Boulbes, N., Bourlès, D., Helvacı, C., Lebatard, A.-E., Mayda, S., Michaud, H., Moigne, A.-M., Nomade, S., Perrin, M., Ponel, P., Rambeau, C., Vialet, A., Gambin, B., and Alçiçek, M. C.: Continuous presence of proto-cereals in Anatolia since 2.3 Ma, and their possible co-evolution with large herbivores and hominins, Sci Rep, 11, 8914, https://doi.org/10.1038/s41598-021-86423-8, 2021.

Athanasiou, M., Bouloubassi, I., Gogou, A., Klein, V., Dimiza, M. D., Parinos, C., Skampa, E., and Triantaphyllou, M. V.: Sea surface temperatures and environmental conditions during the "warm Pliocene" interval (~ 4.1–3.2 Ma) in the Eastern Mediterranean (Cyprus), Global and Planetary Change, 150, 46–57, https://doi.org/10.1016/j.gloplacha.2017.01.008, 2017.

Basilici, G.: Sedimentary facies in an extensional and deep-lacustrine depositional system: the Pliocene Tiberino Basin, Central Italy, Sedimentary Geology, 109, 73–94, https://doi.org/10.1016/S0037-0738(96)00056-5, 1997.

Bering, D.: The development of the Neogene and Quaternary intram ontane basins within the Pisidic lake d istrict in S. Anatolia, Newsletters on Stratigraphy, 27–32, https://doi.org/10.1127/nos/1/1971/27, 1971.

Bertini, A.: Pliocene to Pleistocene palynoflora and vegetation in Italy: State of the art, Quaternary International, 225, 5–24, https://doi.org/10.1016/j.quaint.2010.04.025, 2010.

Bertoldi, R., Rio, D., and Thunell, R.: Pliocene-pleistocene vegetational and climatic evolution of the south-central mediterranean, Palaeogeography, Palaeoclimatology, Palaeoecology, 72, 263–275, https://doi.org/10.1016/0031-0182(89)90146-6, 1989.

Bessais, E. and Cravatte, J.: Les écosystèmes végétaux Pliocènes de catalogne méridionale. Variations latitudinales dans le domaine nord-ouest méditerranéen, Geobios, 21, 49–63, https://doi.org/10.1016/S0016-6995(88)80031-7, 1988.

Beug, H.-J.: Leitfaden der Pollenbestimmung für Mitteleuropa und angrenzende Gebiete, Friedrich Pfeil, München, 542 pp., 2004.

Biltekin, D., Popescu, S.-M., Suc, J.-P., Quézel, P., Jiménez-Moreno, G., Yavuz, N., and Çağatay, M. N.: Anatolia: A long-time plant refuge area documented by pollen records over the last 23 million years, Review of Palaeobotany and Palynology, 215, 1–22, https://doi.org/10.1016/j.revpalbo.2014.12.004, 2015.

Blavoux, B., Dubar, M., and Daniel, M.: Indices isotopiques (13C et 18O) d'un important refroidissement du climat à la fin du Pliocène (formation lacustre de Puimoisson, Alpes-de-Haute-Provence, France), Comptes Rendus de l'Académie des Sciences - Series IIA - Earth and Planetary Science, 329, 183–188, https://doi.org/10.1016/S1251-8050(99)80233-X, 1999.

ter Braak, C. J. F. and van Dam, H.: Inferring pH from diatoms: a comparison of old and new calibration methods, Hydrobiologia, 178, 209–223, https://doi.org/10.1007/BF00006028, 1989.

ter Braak, C. J. F. and Juggins, S.: Weighted averaging partial least squares regression (WA-PLS): an improved method for reconstructing environmental variables from species assemblages, Hydrologia, 269, 485–502, https://doi.org/10.1007/978-94-017-3622-0_49, 1993.

Breiman, L.: Random Forests, Machine Learning, 45, 5–32, https://doi.org/10.1023/A:1010933404324, 2001.

Brewer, S., Guiot, J., Sánchez-Goñi, M. F., and Klotz, S.: The climate in Europe during the Eemian: a multi-method approach using pollen data, Quaternary Science Reviews, 27, 2303–2315, https://doi.org/10.1016/j.quascirev.2008.08.029, 2008.

Brierley, C. M., Fedorov, A. V., Liu, Z., Herbert, T. D., Lawrence, K. T., and LaRiviere, J. P.: Greatly Expanded Tropical Warm Pool and Weakened Hadley Circulation in the Early Pliocene, Science, 323, 1714–1718, https://doi.org/10.1126/science.1167625, 2009.

Brown, T. A., Jones, M. K., Powell, W., and Allaby, R. G.: The complex origins of domesticated crops in the Fertile Crescent, Trends in Ecology & Evolution, 24, 103–109, https://doi.org/10.1016/j.tree.2008.09.008, 2009.

Chevalier, M., Davis, B. A. S., Heiri, O., Seppä, H., Chase, B. M., Gajewski, K., Lacourse, T., Telford, R. J., Finsinger, W., Guiot, J., Kühl, N., Maezumi, S. Y., Tipton, J. R., Carter, V. A., Brussel, T., Phelps, L. N., Dawson, A., Zanon, M., Vallé, F., Nolan, C., Mauri, A., de Vernal, A., Izumi, K., Holmström, L., Marsicek, J., Goring, S., Sommer, P. S., Chaput, M., and Kupriyanov, D.: Pollen-based climate reconstruction techniques for late Quaternary studies, Earth-Science Reviews, 210, 103384, https://doi.org/10.1016/j.earscirev.2020.103384, 2020.

Çolak, M. A., Öztaş, B., Özgencil, İ. K., Soyluer, M., Korkmaz, M., Ramírez-García, A., Metin, M., Yılmaz, G., Ertuğrul, S., Tavşanoğlu, Ü. N., Amorim, C. A., Özen, C., Apaydın Yağcı, M., Yağcı, A., Pacheco, J. P., Özkan, K., Beklioğlu, M., Jeppesen, E., and Akyürek, Z.: Increased Water Abstraction and Climate Change Have Substantial Effect on Morphometry, Salinity, and Biotic Communities in Lakes: Examples from the Semi-Arid Burdur Basin (Turkey), Water, 14, 1241, https://doi.org/10.3390/w14081241, 2022.

Colleoni, F., Masina, S., Negri, A., and Marzocchi, A.: Plio–Pleistocene high–low latitude climate interplay: A Mediterranean point of view, Earth and Planetary Science Letters, 319–320, 35–44, https://doi.org/10.1016/j.epsl.2011.12.020, 2012.

Combourieu-Nebout, N., Bertini, A., Russo-Ermolli, E., Peyron, O., Klotz, S., Montade, V., Fauquette, S., Allen, J., Fusco, F., Goring, S., Huntley, B., Joannin, S., Lebreton, V., Magri, D., Martinetto, E., Orain, R., and Sadori, L.: Climate changes in the central Mediterranean and Italian vegetation dynamics since the Pliocene, Review of Palaeobotany and Palynology, 218, 127–147, https://doi.org/10.1016/j.revpalbo.2015.03.001, 2015.

Connor, S. E., Thomas, I., Kvavadze, E. V., Arabuli, G. J., Avakov, G. S., and Sagona, A.: A survey of modern pollen and vegetation along an altitudinal transect in southern Georgia, Caucasus region, Review of Palaeobotany and Palynology, 129, 229–250, https://doi.org/10.1016/j.revpalbo.2004.02.003, 2004.

Cravatte, J. and Suc, J.-P.: Climatic evolution of North-Western Mediterranean area during Pliocene and Early Pleistocene by pollen-analysis and forams of drill Autan 1. Chronostratigraphic correlations., Pollen et Spores, 23, 247–258, 1981.

Cugny, C., Mazier, F., and Galop, D.: Modern and fossil non-pollen palynomorphs from the Basque mountains (western Pyrenees, France): the use of coprophilous fungi to reconstruct pastoral activity, Veget Hist Archaeobot, 19, 391–408, https://doi.org/10.1007/s00334-010-0242-6, 2010.

Davies, C. P. and Fall, P. L.: Modern Pollen Precipitation from an Elevational Transect in Central Jordan and Its Relationship to Vegetation, Journal of Biogeography, 28, 1195–1210, 2001.

Davis, P. H., Cullen, J., and Coode, M. J. E. (Eds.): INTRODUCTION, in: Flora of Turkey and the East Aegean Islands, Volume 1, vol. 1, Edinburgh University Press, 1–26, 1965.

https://doi.org/10.5194/egusphere-2025-174
Preprint. Discussion started: 18 February 2025

Davraz, A., Sener, E., and Sener, S.: Evaluation of climate and human effects on the hydrology and water quality of Burdur Lake, Turkey, Journal of African Earth Sciences, 158, 103569, https://doi.org/10.1016/j.jafrearsci.2019.103569, 2019.

De Schepper, S., Gibbard, P. L., Salzmann, U., and Ehlers, J.: A global synthesis of the marine and terrestrial evidence for glaciation during the Pliocene Epoch, Earth-Science Reviews, 135, 83–102, https://doi.org/10.1016/j.earscirev.2014.04.003, 2014.

De'ath, G.: Boosted trees for ecological modeling and prediction, Ecology, 88, 243–251, https://doi.org/10.1890/0012-9658(2007)88[243:BTFEMA]2.0.CO;2, 2007.

Dervişoğlu, A., Yağmur, N., Fıratlı, E., Musaoğlu, N., and Tanık, A.: Spatio-Temporal Assessment of the Shrinking Lake Burdur, Turkey, IJEGEO, 9, 169–176, https://doi.org/10.30897/ijegeo.1078781, 2022.

Diniz, F.: Etude palynologique du bassin pliocène de Rio Maior (Portugal), Paléobiologie continentale, 14, 259–267, 1984.

Djamali, M., de Beaulieu, J.-L., Campagne, P., Andrieu-Ponel, V., Ponel, P., Leroy, S. A. G., and Akhani, H.: Modern pollen rain–vegetation relationships along a forest–steppe transect in the Golestan National Park, NE Iran, Review of Palaeobotany and Palynology, 153, 272–281, https://doi.org/10.1016/j.revpalbo.2008.08.005, 2009.

Dowsett, H. J. and Cronin, T. M.: High eustatic sea level during the middle Pliocene:Evidence from the southeastern U.S. Atlantic Coastal Plain, Geology, 18, 435–438, https://doi.org/10.1130/0091-7613(1990)018<0435:HESLDT>2.3.CO;2, 1990.

Dugerdil, L., Joannin, S., Peyron, O., Jouffroy-Bapicot, I., Vannière, B., Boldgiv, B., Unkelbach, J., Behling, H., and Ménot, G.: Climate reconstructions based on GDGT and pollen surface datasets from Mongolia and Baikal area: calibrations and applicability to extremely cold–dry environments over the Late Holocene, Clim. Past, 17, 1199–1226, https://doi.org/10.5194/cp-17-1199-2021, 2021.

Elith, J., Leathwick, J. R., and Hastie, T.: A working guide to boosted regression trees, J Anim Ecology, 77, 802–813, https://doi.org/10.1111/j.1365-2656.2008.01390.x, 2008.

El-Moslimany, A. P.: Ecological significance of common nonarboreal pollen: examples from drylands of the Middle East, Review of Palaeobotany and Palynology, 64, 343–350, https://doi.org/10.1016/0034-6667(90)90150-H, 1990.

Ezquerro, L., Muñoz, A., Liesa, C. L., Simón, J. L., and Luzón, A.: Late Neogene to Early Quaternary climate evolution in southwestern Europe from a continental perspective, Global and Planetary Change, 211, 103788, https://doi.org/10.1016/j.gloplacha.2022.103788, 2022.

Faegri, K., Kaland, P. E., and Krzywinski, K.: Textbook of pollen analysis, John Wiley & Sons, Chichester, 1989.

Fauquette, S., Guiot, J., and Suc, J.-P.: A method for climatic reconstruction of the Mediterranean Pliocene using pollen data, Palaeogeography, Palaeoclimatology, Palaeoecology, 144, 183–201, https://doi.org/10.1016/S0031-0182(98)00083-2, 1998a.

Fauquette, S., Quézel, P., Guiot, J., and Suc, J.-P.: Signification bioclimatiquede taxons-guides du Pliocène méditerranéen, Geobios, 31, 151–169, https://doi.org/10.1016/S0016-6995(98)80035-1, 1998b.

Fauquette, S., Suc, J.-P., Guiot, J., Diniz, F., Feddi, N., Zheng, Z., Bessais, E., and Drivaliari, A.: Climate and biomes in the West Mediterranean area during the Pliocene, Palaeogeography, Palaeoclimatology, Palaeoecology, 152, 15–36, https://doi.org/10.1016/S0031-0182(99)00031-0, 1999.

Fauquette, S., Suc, J.-P., Bertini, A., Popescu, S.-M., Warny, S., Bachiri Taoufiq, N., Perez Villa, M.-J., Chikhi, H., Feddi, N., Subally, D., Clauzon, G., and Ferrier, J.: How much did climate force the Messinian salinity crisis? Quantified climatic conditions from pollen records in the Mediterranean region, Palaeogeography, Palaeoclimatology, Palaeoecology, 238, 281–301, https://doi.org/10.1016/j.palaeo.2006.03.029, 2006.

Fauquette, S., Suc, J. P., Jimenez-Moreno, G., Micheels, A., Jost, A., Favre, E., Bachiri, N., Bertini, T. A., Clet-Pellerin, M., Diniz, F., Farjanel, G., Feddi, N., and Zheng, Z.: Latitudinal climatic gradients in the Western European and Mediterranean regions from the Mid-Miocene (c. 15 Ma) to the Mid-Pliocene (c. 3.5 Ma) as quantified from pollen data, in: Deep-Time Perspectives on Climate Change: Marrying the Signal from Computer Models and Biological Proxies, edited by: Williams, M., Haywood, A. M., Gregory, F. J., and Schmidt, D. N., The Geological Society of London on behalf of The Micropalaeontological Society, 481–502, https://doi.org/10.1144/TMS002.22, 2007.

Feddi, N., Fauquette, S., and Suc, J.-P.: Histoire plio-pléistocène des écosystèmes végétaux de Méditerranée sud-occidentale : apport de l'analyse pollinique de deux sondages en mer d'Alboran, Geobios, 44, 57–69, https://doi.org/10.1016/j.geobios.2010.03.007, 2011.

Fedorov, A. V., Brierley, C. M., Lawrence, K. T., Liu, Z., Dekens, P. S., and Ravelo, A. C.: Patterns and mechanisms of early Pliocene warmth, Nature, 496, 43–49, https://doi.org/10.1038/nature12003, 2013.

Feng, R., Bhattacharya, T., Otto-Bliesner, B. L., Brady, E. C., Haywood, A. M., Tindall, J. C., Hunter, S. J., Abe-Ouchi, A., Chan, W.-L., Kageyama, M., Contoux, C., Guo, C., Li, X., Lohmann, G., Stepanek, C., Tan, N., Zhang, Q., Zhang, Z., Han, Z., Williams, C. J. R., Lunt, D. J., Dowsett, H. J., Chandan, D., and Peltier, W. R.: Past terrestrial hydroclimate sensitivity controlled by Earth system feedbacks, Nat Commun, 13, 1306, https://doi.org/10.1038/s41467-022-28814-7, 2022.

Ge, Y., Li, Y., Bunting, M. J., Li, B., Li, Z., and Wang, J.: Relation between modern pollen rain, vegetation and climate in northern China: Implications for quantitative vegetation reconstruction in a steppe environment, Science of The Total Environment, 586, 25–41, https://doi.org/10.1016/j.scitotenv.2017.02.027, 2017.

Gostyńska, J., Pankiewicz, R., Romanowska-Duda, Z., and Messyasz, B.: Overview of Allelopathic Potential of Lemna minor L. Obtained from a Shallow Eutrophic Lake, Molecules, 27, 3428, https://doi.org/10.3390/molecules27113428, 2022.

Grimm, E. C.: CONISS: a FORTRAN 77 program for stratigraphically constrained cluster analysis by the method of incremental sum of squares, Computers & Geosciences, 13, 13–35, https://doi.org/10.1016/0098-3004(87)90022-7, 1987.

Guiot, J.: Methodology of the last climatic cycle reconstruction in France from pollen data, Palaeogeography, Palaeoclimatology, Palaeoecology, 80, 49–69, https://doi.org/10.1016/0031-0182(90)90033-4, 1990.

Gürel, A. and Yıldız, A.: Diatom communities, lithofacies characteristics and paleoenvironmental interpretation of Pliocene diatomite deposits in the Ihlara–Selime plain (Aksaray, Central Anatolia, Turkey), Journal of Asian Earth Sciences, 30, 170–180, https://doi.org/10.1016/j.jseaes.2006.07.015, 2007.

Haywood, A. M., Dowsett, H. J., Valdes, P. J., Lunt, D. J., Francis, J. E., and Sellwood, B. W.: Introduction. Pliocene climate, processes and problems, Phil. Trans. R. Soc. A., 367, 3–17, https://doi.org/10.1098/rsta.2008.0205, 2009.

https://doi.org/10.5194/egusphere-2025-174
Preprint. Discussion started: 18 February 2025

Haywood, A. M., Hill, D. J., Dolan, A. M., Otto-Bliesner, B. L., Bragg, F., Chan, W.-L., Chandler, M. A., Contoux, C., Dowsett, H. J., Jost, A., Kamae, Y., Lohmann, G., Lunt, D. J., Abe-Ouchi, A., Pickering, S. J., Ramstein, G., Rosenbloom, N. A., Salzmann, U., Sohl, L., Stepanek, C., Ueda, H., Yan, Q., and Zhang, Z.: Large-scale features of Pliocene climate: results from the Pliocene Model Intercomparison Project, Climate of the Past, 9, 191–209, https://doi.org/10.5194/cp-9-191-2013, 2013.

Haywood, A. M., Dowsett, H. J., and Dolan, A. M.: Integrating geological archives and climate models for the mid-Pliocene warm period, Nat Commun, 7, 10646, https://doi.org/10.1038/ncomms10646, 2016.

Haywood, A. M., Tindall, J. C., Dowsett, H. J., Dolan, A. M., Foley, K. M., Hunter, S. J., Hill, D. J., Chan, W.-L., Abe-Ouchi, A., Stepanek, C., Lohmann, G., Chandan, D., Peltier, W. R., Tan, N., Contoux, C., Ramstein, G., Li, X., Zhang, Z., Guo, C., Nisancioglu, K. H., Zhang, Q., Li, Q., Kamae, Y., Chandler, M. A., Sohl, L. E., Otto-Bliesner, B. L., Feng, R., Brady, E. C., von der Heydt, A. S., Baatsen, M. L. J., and Lunt, D. J.: The Pliocene Model Intercomparison Project Phase 2: large-scale climate features and climate sensitivity, Climate of the Past, 16, 2095–2123, https://doi.org/10.5194/cp-16-2095-2020, 2020.

Herbert, T. D., Ng, G., and Cleaveland Peterson, L.: Evolution of Mediterranean sea surface temperatures 3.5–1.5 Ma: Regional and hemispheric influences, Earth and Planetary Science Letters, 409, 307–318, https://doi.org/10.1016/j.epsl.2014.10.006, 2015.

Herzschuh, U., Tarasov, P., Wünnemann, B., and Hartmann, K.: Holocene vegetation and climate of the Alashan Plateau, NW China, reconstructed from pollen data, Palaeogeography, Palaeoclimatology, Palaeoecology, 211, 1–17, https://doi.org/10.1016/j.palaeo.2004.04.001, 2004.

Hijmans, R. J., Phillips, S., and Elith, J. L. and J.: dismo: Species Distribution Modeling, 2021.

Hilgen, F. J., Lourens, L. J., Van Dam, J. A., Beu, A. G., Boyes, A. F., Cooper, R. A., Krijgsman, W., Ogg, J. G., Piller, W. E., and Wilson, D. S.: Chapter 29 - The Neogene Period, in: The Geologic Time Scale, edited by: Gradstein, F. M., Ogg, J. G., Schmitz, M. D., and Ogg, G. M., Elsevier, Boston, 923–978, https://doi.org/10.1016/B978-0-444-59425-9.00029-9, 2012.

Horowitz, A.: Palynological evidence for the Quaternary rates of accumulation along the Dead Sea Rift, and structural implications, Tectonophysics, 164, 63–71, https://doi.org/10.1016/0040-1951(89)90234-5, 1989.

Jankovská, V. and Komárek, J.: Indicative value ofPediastrum and other coccal green algae in palaeoecology, Folia Geobot, 35, 59–82, https://doi.org/10.1007/BF02803087, 2000.

Jiménez-Moreno, G. and Suc, J.-P.: Middle Miocene latitudinal climatic gradient in Western Europe: Evidence from pollen records, Palaeogeography, Palaeoclimatology, Palaeoecology, 253, 208–225, https://doi.org/10.1016/j.palaeo.2007.03.040, 2007.

Jiménez-Moreno, G., Popescu, S.-M., Ivanov, D., and Suc, J.-P.: Neogene flora, vegetation and climate dynamics in southeastern Europe and the northeastern Mediterranean, in: Deep-Time Perspectives on Climate Change: Marrying the Signal from Computer Models and Biological Proxies, vol. 2, edited by: Williams, M., Haywood, A. M., Gregory, F. J., and Schmidt, D. N., Geological Society of London, 0, https://doi.org/10.1144/TMS002.23, 2007.

Jiménez-Moreno, G., Fauquette, S., and Suc, J.-P.: Vegetation, climate and palaeoaltitude reconstructions of the Eastern Alps during the Miocene based on pollen records from Austria, Central Europe, Journal of Biogeography, 35, 1638–1649, https://doi.org/10.1111/j.1365-2699.2008.01911.x, 2008.

Jiménez-Moreno, G., Fauquette, S., and Suc, J.-P.: Miocene to Pliocene vegetation reconstruction and climate estimates in the Iberian Peninsula from pollen data, Review of Palaeobotany and Palynology, 162, 403–415, https://doi.org/10.1016/j.revpalbo.2009.08.001, 2010.

Jiménez-Moreno, G., Alçiçek, H., Alçiçek, M. C., Ostende, L. van den H., and Wesselingh, F. P.: Vegetation and climate changes during the late Pliocene and early Pleistocene in SW Anatolia, Turkey, Quaternary Research, 84, 448–456, https://doi.org/10.1016/j.yqres.2015.09.005, 2015.

Jiménez-Moreno, G., Anderson, R. S., Ramos-Román, M. J., Camuera, J., Mesa-Fernández, J. M., García-Alix, A., Jiménez-Espejo, F. J., Carrión, J. S., and López-Avilés, A.: The Holocene *Cedrus* pollen record from Sierra Nevada (S Spain), a proxy for climate change in N Africa, Quaternary Science Reviews, 242, 106468, https://doi.org/10.1016/j.quascirev.2020.106468, 2020.

Joly, C., Barillé, L., Barreau, M., Mancheron, A., and Visset, L.: Grain and annulus diameter as criteria for distinguishing pollen grains of cereals from wild grasses, Review of Palaeobotany and Palynology, 146, 221–233, https://doi.org/10.1016/j.revpalbo.2007.04.003, 2007.

Juggins, S.: Analysis of Quaternary Science Data. R package version 0.9-26., 2020.

Karas, C., Nürnberg, D., Bahr, A., Groeneveld, J., Herrle, J. O., Tiedemann, R., and deMenocal, P. B.: Pliocene oceanic seaways and global climate, Sci Rep, 7, 39842, https://doi.org/10.1038/srep39842, 2017.

Komárek, J. and Marvan, P.: Morphological Differences in Natural Populations of the Genus *Botryococcus* (Chlorophyceae), Archiv für Protistenkunde, 141, 65–100, https://doi.org/10.1016/S0003-9365(11)80049-7, 1992.

Komárek, J. I. and Jankovská, V.: Review of the Green Algal Genus Pediastrum: Implication for Pollen-analytical Research, , 1–127, 2001.

Kottek, M., Grieser, J., Beck, C., Rudolf, B., and Rubel, F.: World Map of the Köppen-Geiger climate classification updated, metz, 15, 259–263, https://doi.org/10.1127/0941-2948/2006/0130, 2006.

Koutsodendris, A., Allstädt, F. J., Kern, O. A., Kousis, I., Schwarz, F., Vannacci, M., Woutersen, A., Appel, E., Berke, M. A., Fang, X., Friedrich, O., Hoorn, C., Salzmann, U., and Pross, J.: Late Pliocene vegetation turnover on the NE Tibetan Plateau (Central Asia) triggered by early Northern Hemisphere glaciation, Global and Planetary Change, 180, 117–125, https://doi.org/10.1016/j.gloplacha.2019.06.001, 2019.

Kristiansen, J. and Škaloud, P.: Chrysophyta, in: Handbook of the Protists, edited by: Archibald, J. M., Simpson, A. G. B., and Slamovits, C. H., Springer International Publishing, Cham, 331–366, https://doi.org/10.1007/978-3-319-28149-0_43, 2017.

Kuzucuoğlu, C.: The Physical Geography of Turkey: An Outline, in: Landscapes and Landforms of Turkey, edited by: Kuzucuoğlu, C., Çiner, A., and Kazancı, N., Springer International Publishing, Cham, 7–15, https://doi.org/10.1007/978-3-030-03515-0_2, 2019.

https://doi.org/10.5194/egusphere-2025-174
Preprint. Discussion started: 18 February 2025

Lê, S., Josse, J., and Husson, F.: FactoMineR: An R Package for Multivariate Analysis, Journal of Statistical Software, 25, 1–18, https://doi.org/10.18637/jss.v025.i01, 2008.
Lee, C. M., Van Geel, B., and Gosling, W. D.: On the Use of Spores of Coprophilous Fungi Preserved in Sediments to Indicate Past Herbivore Presence, Quaternary, 5, 30, https://doi.org/10.3390/quat5030030, 2022.
Li, Y., Xu, Q., Yang, X., Chen, H., and Lu, X.: Pollen-vegetation relationship and pollen preservation on the Northeastern Qinghai-Tibetan Plateau, Grana, 44, 160–171, https://doi.org/10.1080/00173130500230608, 2005.
Li, Y., Bunting, M. J., Xu, Q., Jiang, S., Ding, W., and Hun, L.: Pollen–vegetation–climate relationships in some desert and desert-steppe communities in northern China, The Holocene, 21, 997–1010, https://doi.org/10.1177/0959683611400202, 2011.
Liaw, A. and Wiener, M.: Classification and Regression by randomForest, 2, 5, 2002.
Lisiecki, L. E. and Raymo, M. E.: A Pliocene-Pleistocene stack of 57 globally distributed benthic δ18O records, Paleoceanography, 20, https://doi.org/10.1029/2004PA001071, 2005.
Lytle, D. E. and Wahl, E. R.: Palaeoenvironmental reconstructions using the modern analogue technique: the effects of sample size and decision rules, The Holocene, 15, 554–566, https://doi.org/10.1191/0959683605hl830rp, 2005.
Ma, Y., Liu, K., Sang, Y., Wang, W., Sun, A., and Feng, Z. (Jordan): A Survey of Modern Pollen and Vegetation along a South-North Transect in Mongolia, Journal of Biogeography, 35, 1512–1532, 2008.
Magri, D. and Parra, I.: Late Quaternary western Mediterranean pollen records and African winds, Earth and Planetary Science Letters, 200, 401–408, https://doi.org/10.1016/S0012-821X(02)00619-2, 2002.
Matthiessen, J. and Brenner, W.: Chlorococcalalgen und Dinoflagellaten-Zysten in rezenten Sedimenten des Greifswalder Boddens (südliche Ostsee), Senckenbergiana Maritima, 27, 33–48, 1996.
Medail, F. and Quézel, P.: Hot-Spots Analysis for Conservation of Plant Biodiversity in the Mediterranean Basin, Annals of the Missouri Botanical Garden, 84, 112–127, https://doi.org/10.2307/2399957, 1997.
Miller, K. G., Wright, J. D., Browning, J. V., Kulpecz, A., Kominz, M., Naish, T. R., Cramer, B. S., Rosenthal, Y., Peltier, W. R., and Sosdian, S.: High tide of the warm Pliocene: Implications of global sea level for Antarctic deglaciation, Geology, 40, 407–410, https://doi.org/10.1130/G32869.1, 2012.
Moore, P. D., Webb, J. A., and Collinson, M. E.: Pollen Analysis, Subsequent edition., Blackwell Science Inc, Oxford, 1991.
Mudelsee, M. and Raymo, M. E.: Slow dynamics of the Northern Hemisphere glaciation, Paleoceanography, 20, https://doi.org/10.1029/2005PA001153, 2005.
Muller, S. D., Daoud-Bouattour, A., Fauquette, S., Bottollier-Curtet, M., Rifai, N., Robles, M., Saber, E.-R., El Madihi, M., Moukrim, S., and Rhazi, L.: Holocene history of peatland communities of central Rif (Northern Morocco), Geobios, S0016699522000018, https://doi.org/10.1016/j.geobios.2021.12.001, 2022.
Muñoz, A., Ojeda, J., and Sánchez-Valverde, B.: Sunspot-like and ENSO/NAO-like periodicities in lacustrinelaminated sediments of the Pliocene Villarroya Basin (La Rioja,Spain), Journal of Paleolimnology, 27, 453–463, 2002.
Nakagawa, T., Brugiapaglia, E., Digerfeldt, G., Reille, M., Beaulieu, J. D., and Yasuda, Y.: Dense-media separation as a more efficient pollen extraction method for use with organic sediment/deposit samples: comparison with the conventional method, Boreas, 27, 15–24, https://doi.org/10.1111/j.1502-3885.1998.tb00864.x, 1998.
d'Oliveira, L., Dugerdil, L., Ménot, G., Evin, A., Muller, S. D., Ansanay-Alex, S., Azuara, J., Bonnet, C., Bremond, L., Shah, M., and Peyron, O.: Reconstructing 15 000 years of southern France temperatures from coupled pollen and molecular (branched glycerol dialkyl glycerol tetraether) markers (Canroute, Massif Central), Climate of the Past, 19, 2127–2156, https://doi.org/10.5194/cp-19-2127-2023, 2023.
Özkaptan, M., Kaymakci, N., Langereis, C. G., Gülyüz, E., Arda Özacar, A., Uzel, B., and Sözbilir, H.: Age and kinematics of the Burdur Basin: Inferences for the existence of the Fethiye Burdur Fault Zone in SW Anatolia (Turkey), Tectonophysics, 744, 256–274, https://doi.org/10.1016/j.tecto.2018.07.009, 2018.
Pagani, M., Liu, Z., LaRiviere, J., and Ravelo, A. C.: High Earth-system climate sensitivity determined from Pliocene carbon dioxide concentrations, Nature Geosci, 3, 27–30, https://doi.org/10.1038/ngeo724, 2010.
Panitz, S., Salzmann, U., Risebrobakken, B., De Schepper, S., and Pound, M. J.: Climate variability and long-term expansion of peatlands in Arctic Norway during the late Pliocene (ODP Site 642, Norwegian Sea), Climate of the Past, 12, 1043–1060, https://doi.org/10.5194/cp-12-1043-2016, 2016.
Peyron, O., Bégeot, C., Brewer, S., Heiri, O., Magny, M., Millet, L., Ruffaldi, P., Van Campo, E., and Yu, G.: Late-Glacial climatic changes in Eastern France (Lake Lautrey) from pollen, lake-levels, and chironomids, Quat. res., 64, 197–211, https://doi.org/10.1016/j.yqres.2005.01.006, 2005.
Peyron, O., Goring, S., Dormoy, I., Kotthoff, U., Pross, J., de Beaulieu, J.-L., Drescher-Schneider, R., Vannière, B., and Magny, M.: Holocene seasonality changes in the central Mediterranean region reconstructed from the pollen sequences of Lake Accesa (Italy) and Tenaghi Philippon (Greece), The Holocene, 21, 131–146, https://doi.org/10.1177/0959683610384162, 2011.
Peyron, O., Magny, M., Goring, S., Joannin, S., de Beaulieu, J.-L., Brugiapaglia, E., Sadori, L., Garfì, G., Kouli, K., Ioakim, C., and Combourieu-Nebout, N.: Contrasting patterns of climatic changes during the Holocene across the Italian Peninsula reconstructed from pollen data, Clim. Past, 9, 1233–1252, https://doi.org/10.5194/cp-9-1233-2013, 2013.
Peyron, O., Combourieu-Nebout, N., Brayshaw, D., Goring, S., Andrieu-Ponel, V., Desprat, S., Fletcher, W., Gambin, B., Ioakim, C., Joannin, S., Kotthoff, U., Kouli, K., Montade, V., Pross, J., Sadori, L., and Magny, M.: Precipitation changes in the Mediterranean basin during the Holocene from terrestrial and marine pollen records: a model–data comparison, Clim. Past, 13, 249–265, https://doi.org/10.5194/cp-13-249-2017, 2017.
Pils, G.: Flowers of Turkey: A photo guide, Pemberley Natural History Books., Austria, 448 pp., 2006.
Plancq, J., Grossi, V., Pittet, B., Huguet, C., Rosell-Melé, A., and Mattioli, E.: Multi-proxy constraints on sapropel formation during the late Pliocene of central Mediterranean (southwest Sicily), Earth and Planetary Science Letters, 420, 30–44, https://doi.org/10.1016/j.epsl.2015.03.031, 2015.
Popescu, S.-M.: Late Miocene and early Pliocene environments in the southwestern Black Sea region from high-resolution palynology of DSDP Site 380A (Leg 42B), Palaeogeography, Palaeoclimatology, Palaeoecology, 238, 64–77, https://doi.org/10.1016/j.palaeo.2006.03.018, 2006.

https://doi.org/10.5194/egusphere-2025-174
Preprint. Discussion started: 18 February 2025

Popescu, S.-M., Biltekin, D., Winter, H., Suc, J.-P., Melinte-Dobrinescu, M. C., Klotz, S., Rabineau, M., Combourieu-Nebout, N., Clauzon, G., and Deaconu, F.: Pliocene and Lower Pleistocene vegetation and climate changes at the European scale: Long pollen records and climatostratigraphy, Quaternary International, 219, 152–167, https://doi.org/10.1016/j.quaint.2010.03.013, 2010.

Prasad, A. M., Iverson, L. R., and Liaw, A.: Newer Classification and Regression Tree Techniques: Bagging and Random Forests for Ecological Prediction, Ecosystems, 9, 181–199, https://doi.org/10.1007/s10021-005-0054-1, 2006.

Price, S. P. and Scott, B.: Pliocene Burdur basin, SW Turkey: tectonics, seismicity and sedimentation, Journal of the Geological Society, 148, 345–354, https://doi.org/10.1144/gsjgs.148.2.0345, 1991.

Quézel, P. and Médail, F.: Ecologie et biogéographie des forêts du bassin méditerranéen, Elsevier, 571 pp., 2003.

Ramezani, E.: Pollen–vegetation relationships in the central Caspian (Hyrcanian) forests of northern Iran, Review of Palaeobotany and Palynology, 12, 2013.

Raymo, M. E., Grant, B., Horowitz, M., and Rau, G. H.: Mid-Pliocene warmth: stronger greenhouse and stronger conveyor, Marine Micropaleontology, 27, 313–326, https://doi.org/10.1016/0377-8398(95)00048-8, 1996.

Reille, M.: Reille, Maurice, 1995. Pollen et spores d'Europe et d'Afrique du Nord, Supplément 1 . Éditions du Laboratoire de botanique historique et palynologie, Marseille, 327 p., 800 FF. / Reille, Maurice, 1998. Pollen et spores d'Europe et d'Afrique du Nord, Supplément 2 . Éditions du Laboratoire de botanique historique et palynologie, Marseille, 530 p., 1600 FF., gpq, 52, 0–0, https://doi.org/10.7202/004885ar, 1998.

Robles, M., Peyron, O., Brugiapaglia, E., Ménot, G., Dugerdil, L., Ollivier, V., Ansanay-Alex, S., Develle, A.-L., Tozalakyan, P., Meliksetian, K., Sahakyan, K., Sahakyan, L., Perello, B., Badalyan, R., Colombié, C., and Joannin, S.: Impact of climate changes on vegetation and human societies during the Holocene in the South Caucasus (Vanevan, Armenia): A multiproxy approach including pollen, NPPs and brGDGTs, Quaternary Science Reviews, 277, 107297, https://doi.org/10.1016/j.quascirev.2021.107297, 2022.

Robles, M., Peyron, O., Ménot, G., Brugiapaglia, E., Wulf, S., Appelt, O., Blache, M., Vannière, B., Dugerdil, L., Paura, B., Ansanay-Alex, S., Cromartie, A., Charlet, L., Guédron, S., de Beaulieu, J.-L., and Joannin, S.: Climate changes during the Late Glacial in southern Europe: new insights based on pollen and brGDGTs of Lake Matese in Italy, Climate of the Past, 19, 493–515, https://doi.org/10.5194/cp-19-493-2023, 2023.

Salonen, J. S., Korpela, M., Williams, J. W., and Luoto, M.: Machine-learning based reconstructions of primary and secondary climate variables from North American and European fossil pollen data, Sci Rep, 9, 15805, https://doi.org/10.1038/s41598-019-52293-4, 2019.

Salonen, J. S., Kuosmanen, N., Alsos, I. G., Heintzman, P. D., Rijal, D. P., Schenk, F., Bogren, F., Luoto, M., Philip, A., Piilo, S., Trasune, L., Väliranta, M., and Helmens, K. F.: Uncovering Holocene climate fluctuations and ancient conifer populations: Insights from a high-resolution multi-proxy record from Northern Finland, Global and Planetary Change, 237, 104462, https://doi.org/10.1016/j.gloplacha.2024.104462, 2024.

Salzmann, U., Haywood, A. M., Lunt, D. J., Valdes, P. J., and Hill, D. J.: A new global biome reconstruction and data-model comparison for the Middle Pliocene, Global Ecology and Biogeography, 17, 432–447, https://doi.org/10.1111/j.1466-8238.2008.00381.x, 2008.

Salzmann, U., Dolan, A. M., Haywood, A. M., Chan, W.-L., Voss, J., Hill, D. J., Abe-Ouchi, A., Otto-Bliesner, B., Bragg, F. J., Chandler, M. A., Contoux, C., Dowsett, H. J., Jost, A., Kamae, Y., Lohmann, G., Lunt, D. J., Pickering, S. J., Pound, M. J., Ramstein, G., Rosenbloom, N. A., Sohl, L., Stepanek, C., Ueda, H., and Zhang, Z.: Challenges in quantifying Pliocene terrestrial warming revealed by data–model discord, Nature Clim Change, 3, 969–974, https://doi.org/10.1038/nclimate2008, 2013.

Schwarz, F., Salzmann, U., Cheng, F., Ni, J., Nie, J., Patchett, M. R., Li, X., Li, L., Woodward, J., and Garzione, C.: High altitude Pliocene to Pleistocene vegetation and climate change of the Kunlun Pass Basin, NE Tibetan Plateau, Global and Planetary Change, 223, 104078, https://doi.org/10.1016/j.gloplacha.2023.104078, 2023.

Shatilova, I. I.: The palynological base of stratigraphical subdivision of late cainozoic deposits of the Western Transcaucasus, Review of Palaeobotany and Palynology, 48, 409–414, https://doi.org/10.1016/0034-6667(86)90077-1, 1986.

Smol, J. P.: Chrysophycean microfossils in paleolimnological studies, Palaeogeography, Palaeoclimatology, Palaeoecology, 62, 287–297, https://doi.org/10.1016/0031-0182(88)90058-2, 1988.

Suc, J. P., Bertini, A., Combourieu-Nebout, N., Diniz, F., Leroy, S., Russo-Ermolli, E., Zheng, Z., Bessais, E., and Ferrier, J.: Structure of West Mediterranean vegetation and climate since 5.3 ma, Acta Zoologica Cracoviensia, 38, 1995.

Suc, J.-P.: Origin and evolution of the Mediterranean vegetation and climate in Europe, Nature, 307, 429–432, https://doi.org/10.1038/307429a0, 1984.

Suc, J.-P. and Cravatte, J.: Etude palynologique du Pliocène de Catalogne (Nord-Est de l'Espagne): apports à la connaissance de l'histoire climatique de la Méditerranée occidentale et implications chronostratigraphiques, Paléobiologie continentale, 13, 1–31, 1982.

Suc, J.-P., Popescu, S.-M., Fauquette, S., Bessedik, M., Jiménez-Moreno, G., Taoufiq, N. B., Zheng, Z., Medail, F., and Klotz, S.: Reconstruction of Mediterranean flora, vegetation and climate for the last 23 million years based on an extensive pollen dataset, Ecologia mediterranea, 44, 53, https://doi.org/10.3406/ecmed.2018.2044, 2018.

Tolotti, M., Thies, H., Cantonati, M., Hansen, C. M. E., and Thaler, B.: Flagellate algae (Chrysophyceae, Dinophyceae, Cryptophyceae) in 48 high mountain lakes of the Northern and Southern slope of the Eastern Alps: biodiversity, taxa distribution and their driving variables, Hydrobiologia, 502, 331–348, https://doi.org/10.1023/B:HYDR.0000004291.03882.f7, 2003.

Tweddle, J. C., Edwards, K. J., and Fieller, N. R. J.: Multivariate statistical and other approaches for the separation of cereal from wild Poaceae pollen using a large Holocene dataset, Veget Hist Archaeobot, 14, 15–30, https://doi.org/10.1007/s00334-005-0064-0, 2005.

https://doi.org/10.5194/egusphere-2025-174
Preprint. Discussion started: 18 February 2025

Vaks, A., Woodhead, J., Bar-Matthews, M., Ayalon, A., Cliff, R. A., Zilberman, T., Matthews, A., and Frumkin, A.: Pliocene–Pleistocene climate of the northern margin of Saharan–Arabian Desert recorded in speleothems from the Negev Desert, Israel, Earth and Planetary Science Letters, 368, 88–100, https://doi.org/10.1016/j.epsl.2013.02.027, 2013.

Van Baak, C. G. C., Mandic, O., Lazar, I., Stoica, M., and Krijgsman, W.: The Slanicul de Buzau section, a unit stratotype for the Romanian stage of the Dacian Basin (Plio-Pleistocene, Eastern Paratethys), Palaeogeography, Palaeoclimatology, Palaeoecology, 440, 594–613, https://doi.org/10.1016/j.palaeo.2015.09.022, 2015.

Van Geel, B.: Non-Pollen Palynomorphs, in: Tracking Environmental Change Using Lake Sediments, vol. 3, edited by: Smol, J. P., Birks, H. J. B., Last, W. M., Bradley, R. S., and Alverson, K., Springer Netherlands, Dordrecht, 99–119, https://doi.org/10.1007/0-306-47668-1_6, 2002.

ten Veen, J. H., Boulton, S. J., and Alçiçek, M. C.: From palaeotectonics to neotectonics in the Neotethys realm: The importance of kinematic decoupling and inherited structural grain in SW Anatolia (Turkey), Tectonophysics, 473, 261–281, https://doi.org/10.1016/j.tecto.2008.09.030, 2009.

Wake, L. V. and Hillen, L. W.: Study of a "bloom" of the oil-rich alga Botryococcus braunii in the Darwin River Reservoir, Biotechnology and Bioengineering, 22, 1637–1656, https://doi.org/10.1002/bit.260220808, 1980.

Wei, H. and Zhao, Y.: Surface pollen and its relationships with modern vegetation and climate in the Tianshan Mountains, northwestern China, Veget Hist Archaeobot, 25, 19–27, https://doi.org/10.1007/s00334-015-0530-2, 2016.

Wei, H., Ma, H., Zheng, Z., Pan, A., and Huang, K.: Modern pollen assemblages of surface samples and their relationships to vegetation and climate in the northeastern Qinghai-Tibetan Plateau, China, Review of Palaeobotany and Palynology, 163, 237–246, https://doi.org/10.1016/j.revpalbo.2010.10.011, 2011.

Willcox, G., Buxo, R., and Herveux, L.: Late Pleistocene and early Holocene climate and the beginnings of cultivation in northern Syria, The Holocene, 19, 151–158, https://doi.org/10.1177/0959683608098961, 2009.

Xiao, S., Li, S., Wang, X., Chen, L., and Su, T.: *Cedrus* distribution change: past, present, and future, Ecological Indicators, 142, 109159, https://doi.org/10.1016/j.ecolind.2022.109159, 2022.

Xu, Q., Li, Y., Tian, F., Cao, X., and Yang, X.: Pollen assemblages of tauber traps and surface soil samples in steppe areas of China and their relationships with vegetation and climate, Review of Palaeobotany and Palynology, 153, 86–101, https://doi.org/10.1016/j.revpalbo.2008.07.003, 2009.

Zhang, Y.-J., Duo, L., Pang, Y.-Z., Felde, V. A., Birks, H. H., and Birks, H. J. B.: Modern pollen assemblages and their relationships to vegetation and climate in the Lhasa Valley, Tibetan Plateau, China, Quaternary International, 467, 210–221, https://doi.org/10.1016/j.quaint.2018.01.040, 2018.

Zhao, Y. and Herzschuh, U.: Modern pollen representation of source vegetation in the Qaidam Basin and surrounding mountains, north-eastern Tibetan Plateau, Veget Hist Archaeobot, 18, 245–260, https://doi.org/10.1007/s00334-008-0201-7, 2009.

Zhao, Y., Yu, Z., and Chen, F.: Spatial and temporal patterns of Holocene vegetation and climate changes in arid and semi-arid China, Quaternary International, 194, 6–18, https://doi.org/10.1016/j.quaint.2007.12.002, 2009.

Zhao, Y., Li, Y., Zhang, Z., Fan, B., Zhu, Y., and Zhao, H.: Relationship between modern pollen assemblages and vegetation in the Bashang typical steppe region of North China, Ecological Indicators, 135, 108581, https://doi.org/10.1016/j.ecolind.2022.108581, 2022.

Zheng, Z., Huang, K., Xu, Q., Lu, H., Cheddadi, R., Luo, Y., Beaudouin, C., Luo, C., Zheng, Y., Li, C., Wei, J., and Du, C.: Comparison of climatic threshold of geographical distribution between dominant plants and surface pollen in China, Sci. China Ser. D-Earth Sci., 51, 1107–1120, https://doi.org/10.1007/s11430-008-0080-x, 2008.

Zheng, Z., Wei, J., Huang, K., Xu, Q., Tarasov, P., Luo, C., Beaudouin, C., Deng, Y., Zheng, Y., Luo, Y., Nakagawa, T., Li, C., Yang, S., Peng, H., and Cheddadi, R.: East Asian pollen database: modern pollen distribution and its quantitative relationship with vegetation and climate, Journal of Biogeography, 14, 2014.